cmgh
CELLULAR AND MOLECULAR GASTROENTEROLOGY AND HEPATOLOGY

ORIGINAL RESEARCH

Porcine Esophageal Submucosal Gland Culture Model Shows Capacity for Proliferation and Differentiation

Richard J. von Furstenberg,[1] Joy Li,[1] Christina Stolarchuk,[1] Rachel Feder,[1] Alexa Campbell,[1] Leandi Kruger,[2] Liara M. Gonzalez,[2] Anthony T. Blikslager,[2] Diana M. Cardona,[3] Shannon J. McCall,[3] Susan J. Henning,[4] and Katherine S. Garman[1]

[1]Division of Gastroenterology, Department of Medicine, [3]Department of Pathology, Duke University, Durham, North Carolina; [2]Department of Clinical Sciences, North Carolina State University, College of Veterinary Medicine, Raleigh, North Carolina; [4]Division of Gastroenterology, Department of Medicine, University of North Carolina Chapel Hill, Chapel Hill, North Carolina

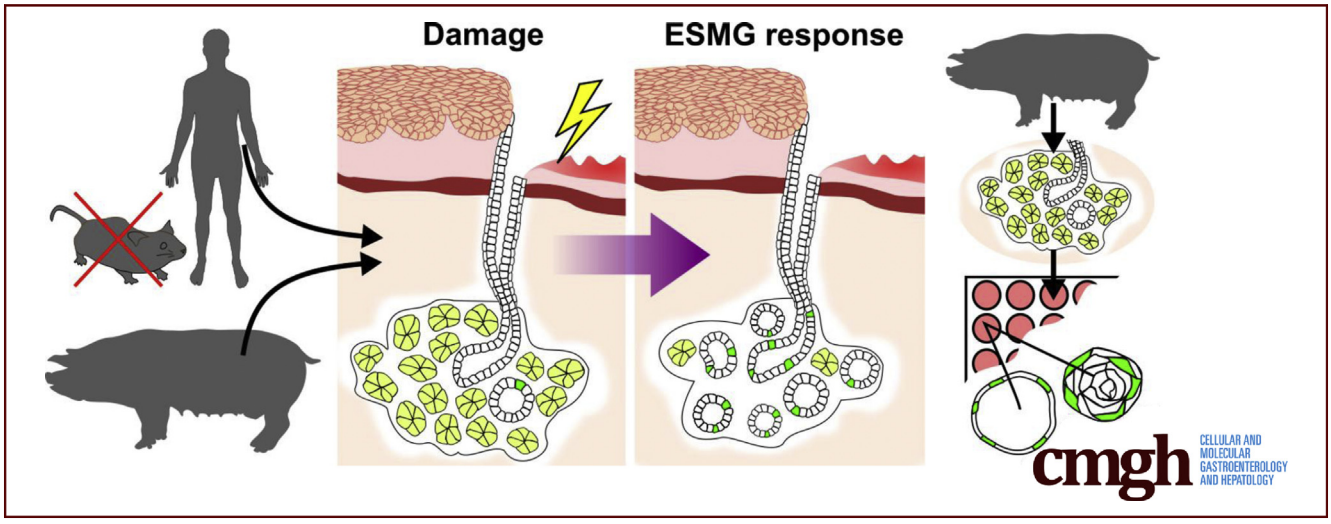

SUMMARY

We describe a novel porcine 3-dimensional culture model that reproduces esophageal submucosal gland proliferation in vivo associated with cancer and injury. Esophageal submucosal glands in culture form 2 different phenotypes of spheroids: one expressing markers of squamous epithelium and the other expressing markers of columnar epithelium.

BACKGROUND & AIMS: Although cells comprising esophageal submucosal glands (ESMGs) represent a potential progenitor cell niche, new models are needed to understand their capacity to proliferate and differentiate. By histologic appearance, ESMGs have been associated with both overlying normal squamous epithelium and columnar epithelium. Our aim was to assess ESMG proliferation and differentiation in a 3-dimensional culture model.

METHODS: We evaluated proliferation in human ESMGs from normal and diseased tissue by proliferating cell nuclear antigen immunohistochemistry. Next, we compared 5-ethynyl-2′-deoxyuridine labeling in porcine ESMGs in vivo before and after esophageal injury with a novel in vitro porcine organoid ESMG model. Microarray analysis of ESMGs in culture was compared with squamous epithelium and fresh ESMGs.

RESULTS: Marked proliferation was observed in human ESMGs of diseased tissue. This activated ESMG state was recapitulated after esophageal injury in an in vivo porcine model, ESMGs assumed a ductal appearance with increased proliferation compared with control. Isolated and cultured porcine ESMGs produced buds with actively cycling cells and passaged to form epidermal growth factor–dependent spheroids. These spheroids were highly proliferative and were passaged multiple times. Two phenotypes of spheroids were identified: solid squamous (P63+) and hollow/ductal (cytokeratin 7+). Microarray analysis showed spheroids to be distinct from parent ESMGs and enriched for columnar transcripts.

CONCLUSIONS: Our results suggest that the activated ESMG state, seen in both human disease and our porcine model, may provide a source of cells to repopulate damaged epithelium in a normal manner (squamous) or abnormally (columnar epithelium). This culture model will allow the evaluation of factors that drive ESMGs in the regeneration of injured epithelium. The raw microarray data have been uploaded to the National Center for Biotechnology Information Gene Expression Omnibus (accession number: GSE100543). *(Cell Mol Gastroenterol Hepatol 2017;4:385–404; http://dx.doi.org/10.1016/j.jcmgh.2017.07.005)*

Keywords: Esophagus; Barrett's Esophagus; 3D Culture; Acinar Ductal Metaplasia; Adult Stem Cell.

Esophageal submucosal glands (ESMGs) are composed of mucous-secreting clusters of cells located within the esophagus beneath the muscularis mucosa. The ESMGs serve a protective role in the esophagus by producing mucins, bicarbonate to neutralize acid, and growth factors, such as epidermal growth factor (EGF). The presence of ESMGs and ducts has been used to anatomically define the tubular esophagus because they are specific to the esophagus and absent from the stomach.[1] Ducts draining the ESMGs are lined by basaloid squamous epithelium and may contain a layer of columnar cells that is either simple or ciliated.[1] Although there is little proliferation of cells within healthy ESMGs in an uninjured esophagus,[2] evidence exists from other glandular gastrointestinal tissues that analogous glands harbor a reserve stem or progenitor cell compartment; this suggests that ESMGs also may be able to respond to esophageal injury.[3] Appropriate ESMG and duct model systems are lacking, however, and, as a result, little is known about the development of the ESMGs and their potential for proliferation and differentiation after injury to the esophageal epithelium.

In human disease, abnormal repair after esophageal injury may result in the development of an intestine-like columnar epithelium known as Barrett's esophagus (BE) rather than normal squamous epithelium.[4] BE is clinically important because of its association with esophageal adenocarcinoma (EAC), a particularly deadly cancer with an overall 5-year survival rate of less than 20%.[5,6] Despite this, the cell of origin for BE remains unknown. Histology shows a close association between ESMGs, their ducts, and overlying epithelium; ESMGs and ducts are present beneath both BE and squamous epithelium.[1] In esophageal resection specimens from human beings, Coad et al[7] described frequent evidence of glands and ducts beneath BE as well as direct histologic continuity of all examined squamous islands with an underlying gland duct. Other histologic studies have shown clusters of ESMGs beneath squamous islands within areas of BE.[8] ESMGs also were identified in patients with BE at the junction between the proximal squamous epithelium and the BE.[8] Importantly, studies of clonality in the esophagus found that a p16 mutation present in a squamous duct from an ESMG also was present in contiguous BE, whereas squamous islands in BE were contiguous with wild-type ESMG ducts.[9] In addition to the notable clonality assay linking ESMG ducts with columnar epithelium, using a different approach, culture of whole human biopsy samples of squamous epithelium and underlying ESMGs showed loss of squamous mucosa and fusion of ESMGs with the surface of the biopsy sample with generation of a single-cell columnar mucosa at 48 hours.[10] The in vivo clonality studies and these short-term whole-biopsy culture findings suggest a role of ESMGs in both repair of squamous epithelium as well as pathogenesis of BE.

Other evidence for a potential role for ESMGs in esophageal epithelial repair comes from an altered histologic appearance of ESMGs in association with esophageal ulcer and esophageal cancer. Specifically, our group has described acinar ductal metaplasia within ESMGs in association with both esophageal injury and esophageal cancer.[11] In acinar ductal metaplasia, rather than containing the mucin-producing acini that characterize normal ESMGs, groups of cells within ESMGs assume a dilated ductal appearance and express the ductal marker cytokeratin 7 (CK7). In other organs such as the pancreas, acinar ductal metaplasia is considered an early event in the progression to cancer.[12,13] However, the functional relationship between acinar ductal metaplasia in ESMGs and the development of BE and EAC is unknown. Similarly, little is known about potential stem cell populations within the protected niche of the ESMGs.

A major limitation to the study of ESMGs has been the lack of traditional rodent models because ESMGs are not found in the mouse esophagus.[14] As a consequence, what is known about ESMGs has resulted from human and atypical animal models. Human studies have shown that at baseline, there appears to be little proliferation of cells within healthy ESMGs. In human patients who were administered the thymidine analog bromodeoxyuridine an hour before undergoing esophagectomy, proliferating cells were identified in the squamous epithelium.[2] The proliferative response of the ESMGs and ducts in the context of esophageal injury has not yet been reported in human beings. However, there was no evidence of proliferation within ESMGs in the esophagus under normal conditions.[2] A similar study identified iododeoxyuridine-positive cells in the basal layer of the squamous epithelium and in the base to the midgland of BE.[15]

In an attempt to bridge the gap between various histologic observations of ESMGs and behavior in vitro, we developed a porcine 3-dimensional (3D) culture model of ESMGs that allows investigators to directly study the proliferative ability of ESMGs. We hypothesized that ESMGs contain reserve progenitor cells that become proliferative after damage and can generate both columnar and squamous epithelium. To this end, we first identified proliferation in human ESMGs in the context of acinar ductal metaplasia. Proliferation in the porcine 3D organoid model then was compared with proliferation in vivo after esophageal injury. Furthermore, in the in vitro system, we identified 2 phenotypes of outgrowths from ESMGs and evaluated these for similarities to the known esophageal epithelial types: normal squamous epithelium and columnar epithelium. ESMG spheroids were further characterized

Abbreviations used in this paper: **ANOVA, analysis of variance; BE, Barrett's esophagus; CK7, cytokeratin 7; DMSO, dimethyl sulfoxide; EAC, esophageal adenocarcinoma; EdU, 5-ethynyl-2′-deoxyuridine; EGF, epidermal growth factor; ESMG, esophageal submucosal gland; IHC, immunohistochemistry; PBS, phosphate-buffered saline; PCNA, proliferating cell nuclear antigen; RFA, radiofrequency ablation; 3D, 3-dimensional.**

Most current article

2352-345X
http://dx.doi.org/10.1016/j.jcmgh.2017.07.005

using microarray analysis to compare gene expression and pathway activity between ESMG spheroids and both freshly dissected ESMGs and squamous tissue.

Materials and Methods

Human and Porcine Tissue for Immunohistochemistry

Human and porcine tissues were compared to assess the histologic appearance of ESMGs and patterns of CK7 and P63 expression. By using a database of human esophagectomy cases and autopsy controls, cases of BE and normal controls were identified as described previously.[11] From this database, archived paraffin-embedded esophageal tissue was obtained under an existing institutional review board protocol. To confirm previous reports of P63 staining in human squamous epithelium,[16–18] 7 cases of BE or EAC were evaluated. Serial sections of an esophageal specimen from a 69-year-old woman with BE containing high-grade dysplasia were used for the examples of CK7 and P63 immunohistochemistry (IHC) as shown in Figure 1*B* and *C*. Sections of autopsy controls and human ESMGs with acinar ductal metaplasia were used to assess proliferation by proliferating cell nuclear antigen (PCNA) staining, as shown in Figure 2.

Porcine esophagus for IHC was collected from Yorkshire Cross pigs purchased from the Swine Educational Unit, Department of Animal Science, North Carolina State University (Raleigh, NC) and housed at North Carolina State University in accordance with both Duke University and North Carolina State University Institutional Animal Care and Use Committee approved protocols. An endoscopic porcine radiofrequency ablation (RFA) model was developed to create injury to esophageal epithelium similar to the procedure used in human beings[19] and adapted for research purposes as previously described by our group.[20] Porcine esophageal tissue from both uninjured and 7-day post-esophageal injury animals was used for IHC. Uninjured and injured porcine esophageal tissue was formalin-fixed and placed in paraffin blocks. Serial sections were cut and prepared under the same protocol that was used for creating sections of human esophagus.

Immunohistochemistry and Immunofluorescence for 5-Ethynyl-2′-Deoxyuridine

CK7 immunohistochemistry was performed as previously reported.[11] Slides were pretreated to remove paraffin and rehydrate with sequential washes in 100% xylene, 100% ethanol, 95% ethanol, 3% hydrogen

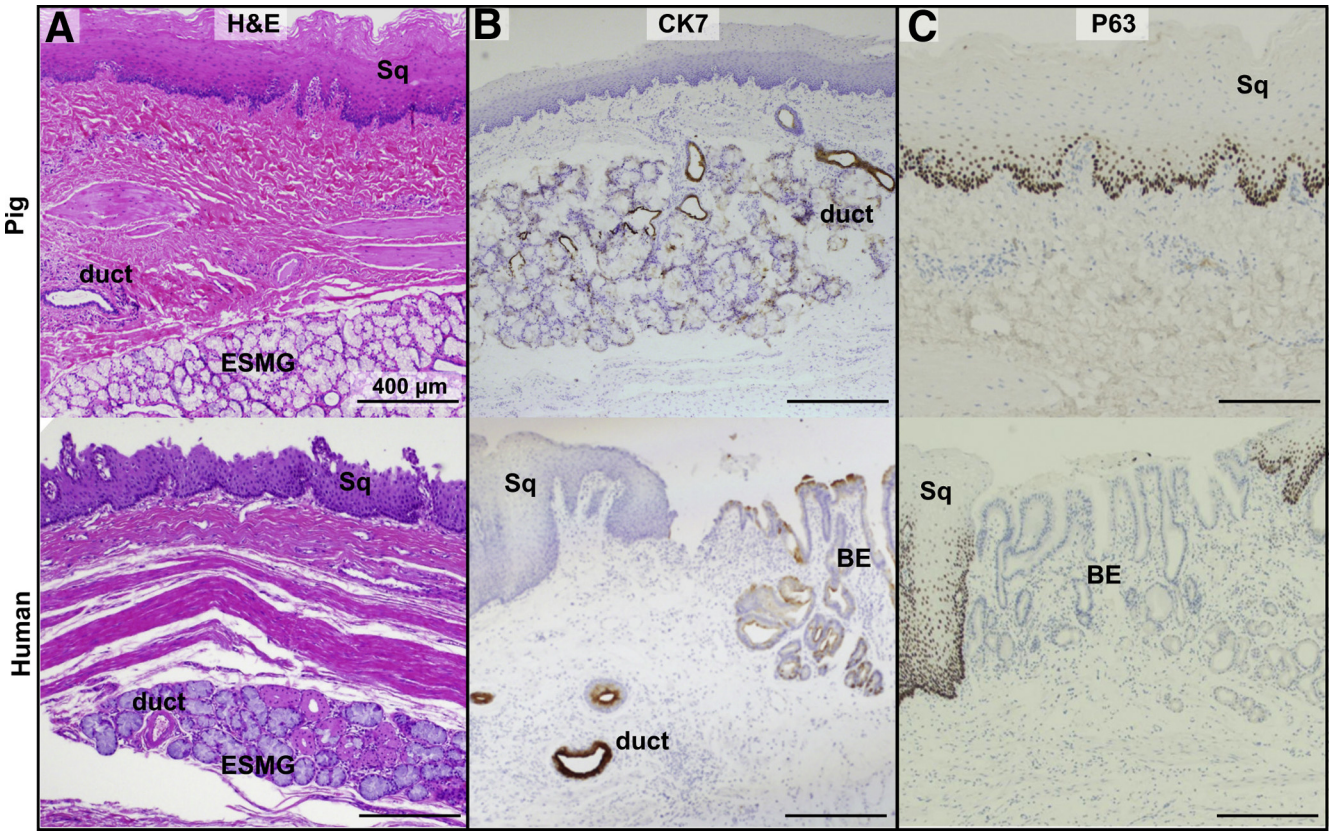

Figure 1. Similarity of porcine and human esophagus. (*A*) Pig (*top row*) and human (*bottom row*) esophagus both contain ESMGs and share overall architecture as shown by H&E staining. (*B*) The CK7 antibody labels the columnar ductal epithelium in pigs, and in human beings the CK7 antibody labels ducts and BE. (*C*) Conversely, P63 antibody marks squamous (Sq) epithelium in pigs and human beings, most strongly in the basal squamous layer. An absence of P63 can be seen in the BE patch of the human tissue.

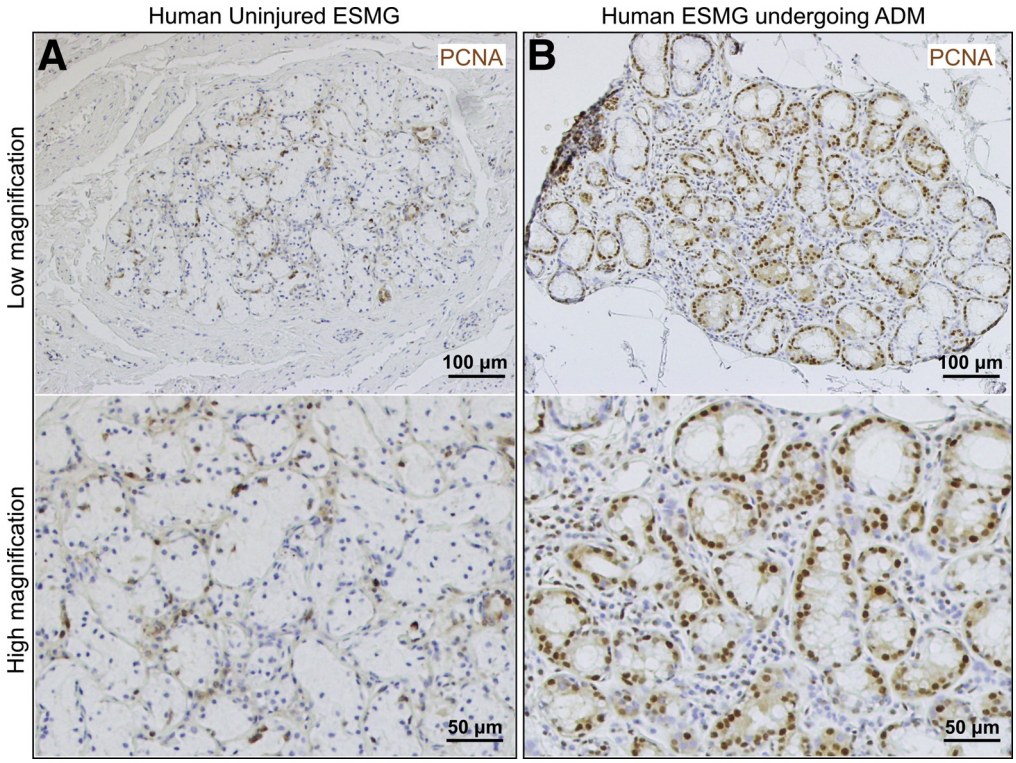

Figure 2. Human ESMGs show proliferation in association with acinar ductal metaplasia (ADM). (*A*) A normal ESMG from a human autopsy case without overlying esophageal injury or cancer shows little proliferation at baseline as shown by proliferating cell nuclear antigen staining. (*B*) An abnormal ESMG from a human esophagectomy case with esophageal adenocarcinoma shows the ductular phenotype within the ESMG with a marked increase in PCNA staining for proliferation.

peroxide in methanol, 95% ethanol, 75% ethanol, deionized water, and Tris-buffered saline. For CK7, pepsin retrieval involved direct application of 300–500 μL of Digest-All (Thermo Fisher, Waltham, MA) for 8–10 minutes at 35°C. After antigen retrieval, protein blocking (Dako, Carpinteria, CA) was performed for 30 minutes at room temperature. CK7 antibody (Dako) was applied at 1:1000 dilution for 1 hour at room temperature. For antibody detection, slides were washed in Tris-buffered saline, and horseradish peroxidase anti-mouse solution was applied at 1× (Dako). Detection was performed with diaminobenzidine (Dako), and counterstaining was performed with hematoxylin solution and bluing agent. Dehydration then was performed with 75% ethanol, 95% ethanol, 100% ethanol, and 100% xylene. The P63 antibody (Biocare Medical, Parcheco, CA) was detected using the Leica Bond system (Leica, Buffalo Grove, IL). Antigen retrieval was performed using Epitope Retrieval 2 solution (Leica), pH 8.9–9.1, for 20 minutes. Antigen detection was performed using Bond Polymer Refine Horseradish Peroxidase Detection (Leica). For PCNA detection, paraffin was removed and tissue sections were rehydrated as described earlier. Antigen retrieval was performed by heating slides in citrate buffer (10 mmol/L sodium citrate, 0.05% Tween 20, pH 6.0) to 100°C for 20 minutes. Sections were blocked for nonspecific binding (as described earlier) and anti-PCNA (Abcam, Cambridge, United Kingdom) (1:1000) was applied overnight at 4°C. 3,3′-Diaminobenzidine tetra hydrochloride chromogen and hematoxylin were used to visualize the antibody and cell nuclei. An Olympus IX71 microscope was used to evaluate histology slides and the Olympus DP2-BSW digital camera and software were used to capture photomicrographs (Olympus, Center Valley, PA) of histology and CK7 images. The P63 images were obtained on an Olympus BX46 trinocular microscope with a 64-Mp shifting pixel camera (model 15.2; Diagnostic Instruments, Sterling Heights, MI).

To place the in vitro model in the context of in vivo response to injury, proliferating cells in the porcine esophagus were identified after systemic administration of 5-ethynyl-2′-deoxyuridine (EdU; Thermo Fisher) to an uninjured Yorkshire Cross pig as well as to an animal that had recovered for 7 days after RFA esophageal injury. EdU was administered as an intraperitoneal injection (2.5 mg/kg body weight) 2 hours before euthanasia as per a previously established protocol.[21] Esophageal tissue was obtained immediately after euthanasia, kept overnight in 4% paraformaldehyde in phosphate-buffered saline (PBS) at 4°C, then placed in 30% sucrose overnight at 4°C, and frozen in Optimal Cutting Temperature compound (Thermo Fisher). EdU was detected using the Alexa 647 azide included in the Imaging Kit (Thermo Fisher) in 10-μm tissue sections. Sections were protein-blocked (Dako) for 30 minutes at room temperature and the sections then were labeled with CK7 (Dako) 1:1000 primary antibody for 1 hour at room temperature, washed 3 times with PBS, and incubated with anti-mouse Alexa 555 1:500 (Thermo Fisher) secondary antibody for 45 minutes at room temperature. 4′,6-Diamidino-2-phenylindole was used at 5 μg/mL for 30 minutes at room temperature to detect DNA in nuclei as described and included in the aforementioned EdU Imaging Kit. After labeling, the slides

Table 1. Primary Antibodies Used

Antibody	Company	Catalog number	Clone
CK7	Dako	MS-7018	OV-TL 12/30
Horseradish peroxidase anti-mouse	Dako	K4001	N/A
p63 (IHC)	Biocare Medical	CM163C	4A4
PCNA	Abcam	AB15497	Polyclonal
Anti-mouse IgG1 Alexa 555	Thermo Fisher	A21127	Polyclonal
p63 (whole-mount immunofluorescence)	Cell Signaling	13109	DRK8X
Anti-rabbit Alexa 647	Biolegend	406414	Poly4064

were washed 3 times with PBS and protected with a coverslip. Details for antibodies used in these experiments can be found in Table 1 and images are presented in Figure 3.

EdU scoring for in vivo uninjured and injured sections was performed. ESMGs, ducts bridging between ESMGs and overlying epithelium, and regions of squamous epithelium were scored using a combination of automated scoring and manual counting, both in ImageJ software (National Institutes of Health, Bethesda, MD). The squamous layer was scored for a defined segment of 3 layers of cells to include the basal and suprabasal layers. Scoring was performed using replicates of defined anatomic units such as single ESMGs, individual ducts to epithelium, and regions of squamous epithelium along multiple complete and continuous tissue sections using image stitching software integral to the EVOS microscope (Thermo Fisher Scientific, Waltham, MA). The scoring technique was based on previous reports in human tissue in which a ductal phenotype had been reported within ESMGs in association with injury and cancer.[11] The detection of EdU+ nuclei was determined for ESMGs, ducts, and overlying squamous epithelium, whereas 4′,6-diamidino-2-phenylindole was used to count total nuclei. The percentage of EdU+ cells was determined for each structure. Based on our previous findings in human beings, we evaluated the presence of a ductal phenotype within ESMGs. Because we determined that more than 50% of ESMGs in the injured esophagus contained this ductal phenotype, these injury-associated ductal ESMGs were scored for EdU. For the control animal, 14 unique ESMGs were evaluated across 5 distinct tissue section scans, totaling 18,678 ESMG nuclei. In comparison, 15 unique ESMGs from the RFA-treated animal were identified and evaluated from 10 distinct tissue scans of tissue from the area of the previous injury, for a total of 13,507 nuclei. From these same distinct tissue scans described earlier, 18 unique ducts (3593 nuclei total) were evaluated from the control animal and 24 unique ducts (3932 nuclei total) were scored from the RFA-treated animal. Basal squamous cells were evaluated from the squamous layer across 5 unique and complete tissue sections scans from the control (10,428 nuclei total) and RFA-treated animal (11,177 nuclei total). All mean values for these analyses are expressed in the results as means ± SEM. Statistical analysis of control and injured squamous segments, ducts, and ESMGs was performed in Prism 6 software (GraphPad, La Jolla, CA) using the Mann–Whitney *U* test.

Esophageal Tissue for In Vitro 3D Cell Culture

Porcine esophageal tissue for cell culture was obtained from City Packing (Burlington, NC), with permission from the North Carolina Department of Agriculture and Consumer Services. Whole fresh esophagus was collected at the time of processing and transported for approximately 30 minutes in 4°C PBS at pH 7.4 before experiments.

ESMG Harvest and Culture

After delivery to the laboratory, fresh porcine esophagus was prepared for harvest of ESMGs. An illustrated diagram of the ESMG isolation and culture methods is provided in Figure 4. Each esophagus was opened longitudinally with dissection scissors (Figure 4*A*). The esophagus then was washed thoroughly with tap water to remove any contents from the lumen (Figure 4*B*). To expose the submucosa, the epithelium was peeled off of the muscle layers using a combination of sharp and primarily blunt dissection (Figure 4*C*). The epithelial layer was placed with the luminal surface facing down on a dissection board (Figure 4*D*). Loose stromal material was lifted with forceps and removed. ESMGs were dissected carefully out of the submucosa (Figure 4*E*). Particular care was taken to leave the squamous layer intact, including gently lifting ESMGs off the squamous layer with forceps and then removing them and closely inspecting the squamous layer to ensure that it remained without defect. ESMGs were placed in a conical tube of cold PBS after dissection. After collection, the ESMGs then were placed on a smooth hard surface and finely minced with a razor blade until all fragments were less than 1 mm across (Figure 4*F*). This slurry of ESMG fragments was lifted from the surface with a cut pipette tip (for wider opening to facilitate passage of larger fragments) and transferred to a conical tube. Minced ESMGs then were incubated in minimal media of Advanced Dulbecco's modified Eagle medium/F12 (Thermo Fisher) with metronidozole 10 mg/mL (Sigma), antibiotic–antimycotic (Sigma), gentamicin 25 μg/mL (Thermo Fisher), kanamycin 100 μg/mL (Sigma), HEPES 10 mmol/L (Thermo Fisher), and Glutamax 1× (Thermo Fisher) (Figure 3*G*). After 15 minutes at 37°C, dithiothreitol was added (to 3 mmol/L) for an additional 15 minutes of incubation. The slurry from 12 minced glands was spun down at 100 × g and rinsed with minimal media before being resuspended in 480 μL Growth Factor Reduced Matrigel Matrix (Corning, Durham, NC) for a 24-well plate, yielding 20-μL patties of ESMGs in Matrigel (Figure 3*H*). After plating, the Matrigel patties

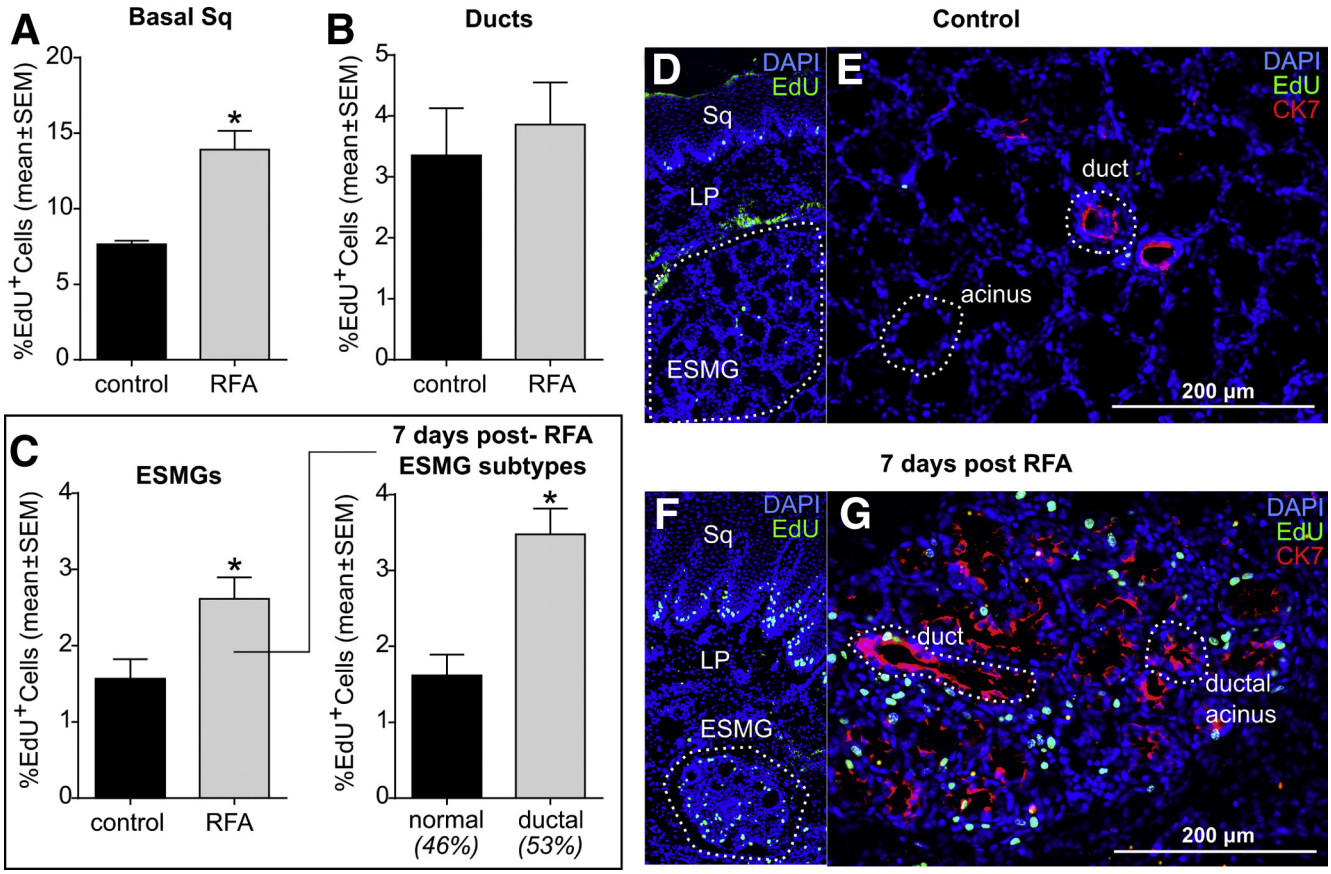

Figure 3. Porcine ESMGs become hyperproliferative with a ductular phenotype after in vivo damage to the overlying epithelium. The percentage of EdU+ nuclei within the basal squamous epithelial layer, ducts, and ESMGs was compared between 2 animals: 1 control and the other 7 days after RFA. (*A*) EdU+ nuclei increased in the basal squamous cells after RFA. (*B*) Ducts did not show a significant increase in proliferation after RFA. (*C*) However, after RFA, activated ESMGs with the ductal phenotype were found in 53% of ESMGs. After injury, activated ESMGs showed significantly more EdU label than control. (*D*) Low-power esophageal tissue section scan from the control animal labeled with EdU azide dye (green) to mark cells in the S-phase and 4′,6-diamidino-2-phenylindole (DAPI; blue) marking all nuclei. The *white dashed border* marks the ESMG perimeter, and the squamous layer and lamina propria are labeled Sq and LP, respectively. (*E*) Higher-power image of an ESMG from the control animal labeled with DAPI (blue), EdU (green), and ductal marker CK7 (red). An example of a duct and acinus are outlined with a *dashed white line*. (*F*) Low-power scan of esophageal section from an animal 7 days after RFA shows an active ESMG with increased proliferation. (*G*) Higher-power image of a representative ESMG from an animal 7 days after RFA, EdU (green), CK7 (red), and DAPI (blue). This ESMG has an activated ductal phenotype with increased CK7 within the ESMG compared with control. An example of a CK7-positive duct and a ductal acinus are marked with *white dashed borders*.

were overlaid with 800 μL minimal media that was changed every 2–3 days.

As a control, squamous epithelium with adherent lamina propria also was dissected and finely minced and treated in a similar fashion to ESMGs. Squamous fragments then were plated in Matrigel and overlaid with media as described earlier. Because ESMGs secrete EGF into the squamous-lined lumen of the esophagus, as an additional control, squamous epithelium also was minced and plated with recombinant human EGF (R&D Systems, Minneapolis, MN) at 5 ng/mL, which approximates the physiologic concentration in human esophagus (range, 1.78–2.14 ng/mL).[22]

At day 7, new growth from minced ESMG fragments was passaged. Matrigel containing EMSG fragments was scraped with a pipette tip, allowing Matrigel to be pooled from the aforementioned 24-well plate into a 50-mL conical tube from each animal-derived cell culture. Conical tubes were chilled on ice for 15 minutes to depolymerize the Matrigel and then vortexed on high 10 times. Then, after centrifugation at 100 $\times$ g for 5 minutes at 4°C, the media was aspirated off, and the pellet was resuspended in 4 mL of Accutase (Stemcell Technologies, Vancouver, Canada) for 45 minutes at 37°C with vortexing every 15 minutes during the incubation. After the incubation, the suspension was pipetted up and down with a serologic pipette 20 times before passing the suspension through a 40-μm filter (Corning) and pelleting the cells at 100 $\times$ g for 5 minutes at 4°C. The Accutase was aspirated off and the pellet was washed with 10 mL of minimal media, spinning down as described earlier. The cells then were counted with a hemocytometer and plated in a 48-well plate at a density of approximately 2000 cells per 10 μL Matrigel, or approximately 500 cells

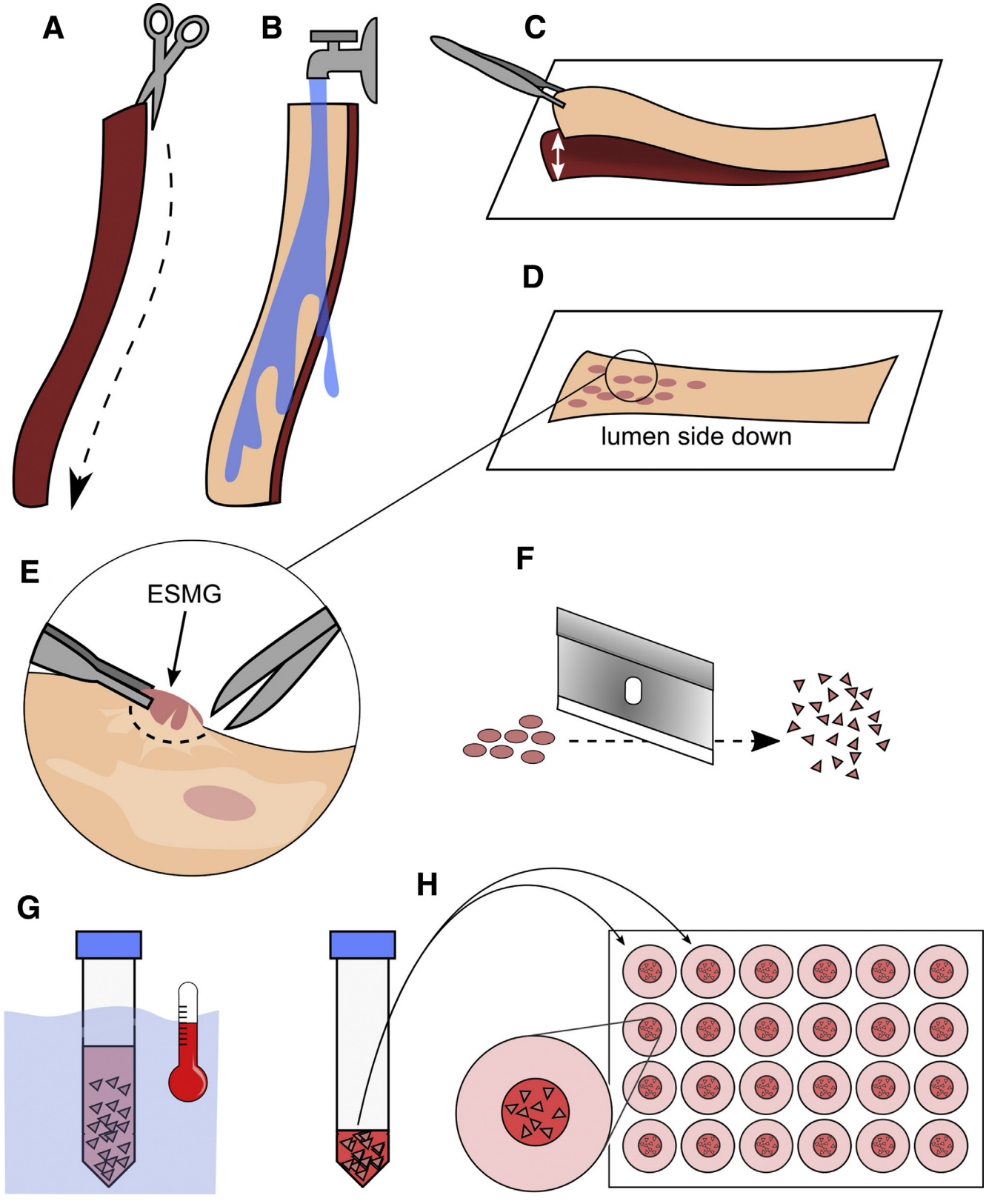

Figure 4. ESMGs are prepared for in vitro 3D culture. (*A*) The esophagus is opened longitudinally. (*B*) Vigorous washing is performed. (*C*) The epithelial layer is peeled off the muscle layers. (*D*) ESMGs are exposed for dissection by placing luminal side down on a dissecting board. (*E*) ESMGs are dissected. (*F*) ESMGs are minced. (*G*) Minced ESMGs are incubated with minimal media and antibiotics (see the Materials and Methods section for details). (*H*) Minced ESMGs are plated into Matrigel for culture.

per 5 μL Matrigel for the EGF titration experiment described later. The Matrigel patties containing these passaged cells were overlaid with 200 μL spheroid media, which is minimal media with the addition of 50 ng/mL recombinant human EGF (R&D Systems), B27–vitamin A Free 1× (Thermo Fisher), and N2 1× (Thermo Fisher). This media formula was used for all spheroid experiments unless otherwise stated.

Passaging from spheroids followed the same process as described earlier for the original growth, with the exception of the Accutase incubation being shortened to 30 minutes at 37°C. To measure spheroid-forming efficiency, three 10-uL Matrigel patties were imaged in their entirety at day 5 with a 4× objective on an EVOS microscope. Spheroids greater than 80 μm were counted and divided by the total number of cells per well as assessed by EVOS image analysis and cell counting software (Thermo Fisher).

For the EGF titration experiment, cells were obtained on their first passage to avoid possible selection for an EGF-dependent subpopulation. Canertinib (CI-1033; Selleckchem, Houston, TX) is an irreversible tyrosine-kinase inhibitor with activity against EGF receptor (median inhibitory concentration, 0.8 nmol/L), HER-2 (median inhibitory concentration, 19 nmol/L), and erb-b2 receptor tyrosine kinase 4 (median inhibitory concentration, 7 nmol/L). To experimentally block the EGF receptor, canertinib (CI-1033; Selleckchem), was dissolved in dimethyl sulfoxide (DMSO) to 1 mmol/L and added at 1000× to spheroid media (with 50 ng/mL EGF) for a final concentration of 1 μmol/L. As a control, DMSO alone without canertinib was added to spheroid media. At day 5, the number of spheroids per well was counted in a blinded fashion. Images of the entire well were captured with a 4× objective for 4 wells from each condition per biological replicate using an EVOS microscope (Thermo Fisher). The images were assigned arbitrary labels, scrambled, and scored by different members of the research team. To be counted as a spheroid, a size cut-off point of larger than 80 μm in diameter was established. Counting was performed using the Cell Counter plugin within ImageJ software. Statistical analysis was performed using a 1-way analysis of variance (ANOVA) with the Tukey multiple comparisons test in Prism 6 software (GraphPad).

Whole-Mount Immunofluorescence

Outgrowths from the minced ESMG fragments were identified by their conspicuous protrusion over time (appearing between days 3 and 5), and their proliferative status was assessed by adding 10 μmol/L EdU to the media for 4 hours on day 7 after plating. Whole-mount labeling using the method described by Wang et al,[23] in combination with the aforementioned EdU Imaging Kit, was used to detect the incorporated EdU.

Whole-mount in situ labeling of spheroids was accomplished in a similar manner using CK7 at 1:1000 (Dako) and P63 at 1:1000 (Cell Signaling, Danvers, MA) primary antibodies, and anti-mouse Alexa 555 1:500 and anti-rabbit Alexa 647 at 1:500 (Biolegend, San Diego, CA) secondary antibodies, respectively. EdU (10 μmol/L) was added to live spheroid media overnight before fixation for whole-mount imaging. EdU+ cells were identified using the aforementioned EdU imaging kit. Images were acquired on an EVOS microscope and fluorescent image merging was performed using ImageJ software. In conjunction with immunofluorescence, phenotype was identified based on a solid or hollow morphology.

Flow Cytometry

Proliferation was evaluated by adding 10 μmol/L EdU to culture media of spheroid cultures from 3 pigs overnight on day 6. On day 7, the spheroids were harvested from one 48-well plate per pig (3 pigs) and digested to single cells using Accutase, as previously mentioned. The cells harvested from 144 wells total (3 pigs) were pooled and the EdU was labeled using the Alexa 488–Flow Cytometry Kit (Thermo Fisher). The percentage of EdU+ cells was measured on a FACSCanto II (BD Biosciences, San Jose, CA).

For the bivariate analysis of CK7 and P63 expression by flow cytometry, spheroid-derived single cells were pooled from separate pigs and fixed with 4% paraformaldehyde for 10 minutes at room temperature, permeabilized with 0.5% Triton X-100 (Thermo Fisher) for 10 minutes at 4°C, blocked with 1% bovine serum albumin in PBS for 30 minutes, incubated with anti-CK7 or anti-P63 1:1000 primary antibodies overnight at 4°C, followed with the same secondary antibodies, concentrations, and conditions described for whole-mount immunofluorescence. All flow cytometry data were analyzed using Summit 4.3 Software (Cytomation, Ft. Collins, CO).

Microarray

Tissues harvested directly from uninjured pigs (age/size) (whole esophagus, squamous tissue, and excised ESMGs) were collected and stored at -20°C in RNA*later* (Thermo Fisher) then removed, homogenized in Qiazol (Qiagen, Germantown, MD) lysis reagent, and processed using the RNeasy Plus Universal Mini Kit (Qiagen). Spheroids were harvested on day 7 after plating using RLT lysis reagent and the RNA was isolated using the RNeasy Micro Kit (Qiagen). For both the aforementioned tissues and spheroids, 3 biological replicates were used in this microarray. RNA quality and concentration were assessed using a 2100 Bioanalyzer (Agilent, Santa Clara, CA) and NanoDrop (Thermo Fisher) spectrophotometer before submission to the Sequencing and Genomic Technologies Core at Duke, where the RNA (200 ng) was used to synthesize fragmented and labeled sense-strand complementary DNA and hybridized onto an Affymetrix (Thermo Fisher) Porcine 1.0 ST Array. Robust multichip analysis normalization was performed on the entire data set. The Affymetrix (Santa Clara, CA) Expression Console and Transcriptome Analysis Console (version 3.0) software was used to analyze gene level differential expression between groups using a 1-way between-subject ANOVA (unpaired). Differentially expressed genes were selected with a cut-off P value of less than .05 based on an ANOVA test and a 2-fold change cut-off value. Of note, the porcine genome annotation has improved

greatly in recent years, although some gaps in microarray annotation remain. For microarray probes in which an LOC identifier was provided without a gene name, a manual search of the porcine genome for the corresponding EntrezGene gene symbol was performed through the National Center for Biotechnology Information, US National Library of Medicine (https://www.ncbi.nlm.nih.gov/gene/) using the June 14, 2017 update for the *Sus scrofa* (pig) genome.

In some cases, the gene loci still was without complete annotation. In these cases, the differentially expressed genes with annotation were included in the analysis. The raw microarray data have been uploaded to the National Center for Biotechnology Information Gene Expression Omnibus (accession number: GSE100543).

Principal component analysis was performed using the Affymetrix Expression Console software. Gene ontology enrichment analysis on the gene lists was performed using the Database for Annotation, Visualization, and Integrated Discovery. To determine gene ontology term enrichment, the proportion of test genes that mapped to a particular gene ontology term was compared with the proportion of genes from the entire GeneChip that mapped to the same term. Enriched biological process and cellular component terms shown had a *P* value and false discovery rate cut-off value of less than .05. The selected regenerative candidate terms in the cross-comparison met the criteria of a *P* value less than .05. To determine important pathways in the ESMGs, a list of the enriched genes (fold change > 2; $P < .05$) were entered into the PANTHER Classification System (version 11.1; University of Southern California, Los Angeles, CA).[24,25] By using the functional classification viewed in the gene list analysis tool, a list of genes was created that then was converted to biologic pathways.

Results

Porcine and Human Esophageal Tissues Contain Similar Structures and Share Markers

For the current studies, we pursued a porcine model given the histologic similarities previously noted between porcine and human ESMGs.[14] When we directly compared human and porcine esophageal histology, we found ESMGs in both species. Figure 1*A* shows basic esophageal histology with an esophageal lumen lined by squamous epithelium several cells thick. Beneath the squamous epithelium, a layer of lamina propria is present and a thin muscularis mucosa is located above the ESMGs. Ducts connect the ESMGs to the esophageal lumen. CK7 is a known marker of BE[26] and also has been reported in ESMGs and ducts.[11,27] In the normal squamous epithelium, however, CK7 is not present.[9,28] When we stained for CK7 expression in human and porcine esophagus (Figure 1*B*), it was prominent in human ESMGs and ducts, as well as in BE. CK7 also was found in porcine ESMGs and ducts. In contrast, P63 is a marker of squamous epithelium that is absent in BE[16–18] and constitutively expressed in squamous epithelium in skin, esophagus, and ectocervix.[16] We detected P63 in the basal layer of squamous epithelium in both porcine and human esophagus, and, as expected, its expression was absent in human BE (Figure 1*C*).

Proliferation in Human ESMGs Is Associated With Acinar Ductal Metaplasia

As previously reported, when autopsy controls were compared with human esophagectomy cases, acinar ductal metaplasia in ESMGs was noted in association with both injury and cancer.[11] By using a subset of the autopsy controls and esophageal cancer cases with acinar ductal metaplasia, we tested the hypothesis that acinar ductal metaplasia in ESMGs would be accompanied by increased proliferation as visualized by PCNA immunolabeling. Figure 2 shows the contrast between representative ESMGs from an uninjured baseline state and an activated proliferative state associated with cancer. The autopsy control ESMG has minimal proliferation with little PCNA staining (Figure 2*A*), whereas the ESMG with acinar ductal metaplasia (Figure 2*B*) shows marked PCNA staining, reflective of increased proliferation. These findings in human ESMGs prompted us to evaluate proliferation in a porcine model after acute injury.

Porcine Esophagus Responds to Injury With Proliferation in ESMGs and Ducts

By using an in vivo porcine model of esophageal epithelial injury and repair by radiofrequency ablation technique, uptake of the thymidine analog EdU 7 days after esophageal injury was evaluated. At this time point, re-epithelialization had begun with formation of a neo-squamous epithelium. EdU-positive cells were counted for areas of squamous epithelium, ducts, and ESMGs for the control and injured animals as shown in Figure 3. When compared with control, the postinjury esophagus contained a new subtype of ESMG with more than 2 ducts within the ESMGs, similar to what we had previously reported in the human esophagus.[11] As expected, the basal layers of squamous epithelium showed a marked increase in EdU in areas adjacent to acute esophageal ulceration with an increase from the baseline labeling index of 7.6% ± 0.3% to a post-injury index of 14% ± 1.2% ($P = .008$) (Figure 3*A*). Labeling in ducts bridging from ESMGs to squamous epithelium was similar in controls (3.4% ± 0.8%) and after injury (3.9% ± 0.7%; $P = .52$). ESMGs in controls showed minimal proliferation, with EdU labeling of 1.6% ± 0.3% cells. After RFA injury, 53% of ESMGs showed an activated phenotype with a ductal appearance; these ductal ESMGs showed double the proliferation compared with normal ESMGs, with increased EdU labeling to 3.5% ± 0.3% of cells ($P = .0001$) (Figure 3*A*). Images of EdU labeling are shown in normal esophagus where a large ESMG is pictured beneath squamous epithelium (Figure 3*B*) and proliferation was rare. In the area adjacent to esophageal injury, more than 50% of ESMGs showed the active phenotype of ESMGs with increased intercalated ducts as shown in Figure 4*C*, where the increase in EdU in the suprabasal layer of squamous epithelium was apparent, as was the increase in EdU in the ESMG. In association with increased proliferation within

ESMGs, there was prominent CK7 expression in ESMGs after injury, illustrating the ductal phenotype in vivo compared with the uninjured control (Figure 3*D* and *E*).

ESMG Proliferation In Vitro After Mincing and Ability to Passage

When ESMGs were carefully dissected from underneath the squamous epithelium, minced, and placed in 3D culture, a population of highly proliferative cells emerged. Detailed methods on this technique are provided in Figure 4. Histologic evaluation of the epithelium that remained after ESMGs were dissected indicated that squamous epithelium was not present in the initial cultures. Figure 5*A* shows the histology of squamous epithelium with intact ESMGs and Figure 5*B* shows squamous epithelium after dissection of the ESMGs. Importantly, the layer of lamina propria that lies between the squamous epithelium and the ESMGs remained with the squamous epithelium and the entire squamous epithelium remained intact. Thus, we concluded that these cultures of ESMGs did not contain proliferative cells known to reside in squamous epithelium.

Although great care was taken to avoid any contamination with squamous epithelium as described earlier (and as shown in Figure 5*B*), as a control experiment, the remnant overlying squamous tissue that remained after the ESMGs had been dissected away was processed in parallel with the ESMGs. ESMGs showed robust outgrowths in culture as shown in Figure 5*C* and *D*. In contrast, culture of squamous tissue showed essentially no growth (Figure 5*C* and *E*). Because ESMGs are known to secrete EGF, to determine whether lack of EGF in squamous culture accounted for the differential growth of ESMGs as compared with the squamous epithelium, the latter cultures were repeated with the addition of EGF. As can be seen in Figure 5*C* and *F*, when EGF was added to squamous culture, no growth was observed.

Within 7 days of initial plating, minced ESMGs in culture produced buds with balloon-like outgrowths as well as solid buds (Figure 6). As shown in Figure 6*A*, these outgrowths were digested into single cells, separating them away from the originating gland fragments that are rich in extracellular matrix. After 5 days, the digested cells formed spheroids with 8.1% ± 0.6% efficiency (Figure 6*C* and *D*). The spheroids could then be further passaged (Figure 6*A*), with efficiency increasing to 72% ± 1% (Figure 6*D*). To date, we have repeated up to 7 passages without an apparent loss of efficiency.

The high efficiency of passaged spheroids from ESMGs clearly implies the presence of proliferating cells. Split ratios during passage are 1:3 or higher, similar to results with intestinal stem cell culture in which self-renewal through repeated passage has been used as evidence of stemness.[29] To quantitate the proportion of proliferating cells in our 3D ESMG culture model, we added the thymidine analog EdU to the spheroid cultures. After an overnight incubation with the analog, spheroids showed marked incorporation of EdU by whole-mount imaging (Figure 6*C*). Flow cytometry of these spheroids digested to single cells showed 64% were positive for EdU, indicating a high level of proliferation 7 days after passage (Figure 6*E*).

ESMG Spheroids Depend on EGF

Given the established role of ESMGs in the esophagus as a source of growth factors such as EGF,[30] we hypothesized that ESMGs would serve as their own niche in culture with minimal media. Indeed, the minced ESMGs generated proliferating outgrowths in culture without the addition of growth factors. However, we found that Matrigel and minimal media alone were not sufficient to drive the proliferative cells when they were passaged away from their originating ESMG fragments. Figure 7 shows that when no EGF was added to the media, there was essentially no progression of single cells into multicellular spheroids. In contrast, with 50 ng/mL EGF, as used in the popular "Sato condition" for intestinal epithelial cell culture,[31] robust spheroid formation resulted. When this EGF concentration was titrated down to the physiologic concentration of 2.5 ng/mL found in esophageal secretions,[30] this robust proliferation and spheroid formation was maintained. The similar proliferative response that occurred even with a substantial decrease in EGF indicates an exquisite EGF sensitivity. To bolster this finding of EGF dependency, EGF's target receptors were blocked with canertinib (CI-1033), an irreversible pan-ErbB tyrosine-kinase inhibitor and experimental drug candidate for the treatment of cancer. When 1 μmol/L canertinib was administered concomitantly with 50 ng/mL EGF, the formation of spheroids was decreased significantly, approximating the result of the no EGF group. When DMSO, the vehicle for canertinib, was added at a 1:1000 dilution with 50 ng/mL EGF, there was a negligible decrease in spheroid number. These results are shown with representative images (Figure 7).

Microarray Analysis Shows Transcriptome of Spheroids to Be Distinct From Originating ESMG Tissue

To globally compare gene expression in cultured porcine ESMGs with both normal squamous epithelium and intact ESMGs, we performed a microarray analysis. In a principal component analysis plot of these data, the cultured ESMGs represented a distinct population from intact ESMGs, squamous epithelium, and whole uninjured porcine esophagus (Figure 8*A*). Given the EdU uptake, and need for frequent passaging in cultured ESMG-derived spheroids, we predicted that the enriched biological processes would be consistent with increased proliferation. Indeed, when we compared the cultured spheroids with freshly dissected ESMGs, there was evidence of increased cell proliferation as well as an increase in cell-cycle markers, hormone responses, and genes associated with gland development. In addition to increased proliferation, spheroids compared with squamous epithelium also showed increased expression of genes related to responses to wound healing (Figure 8*B*). Given the hypothesis that under certain circumstances BE may derive from ESMGs, we identified established BE markers from the

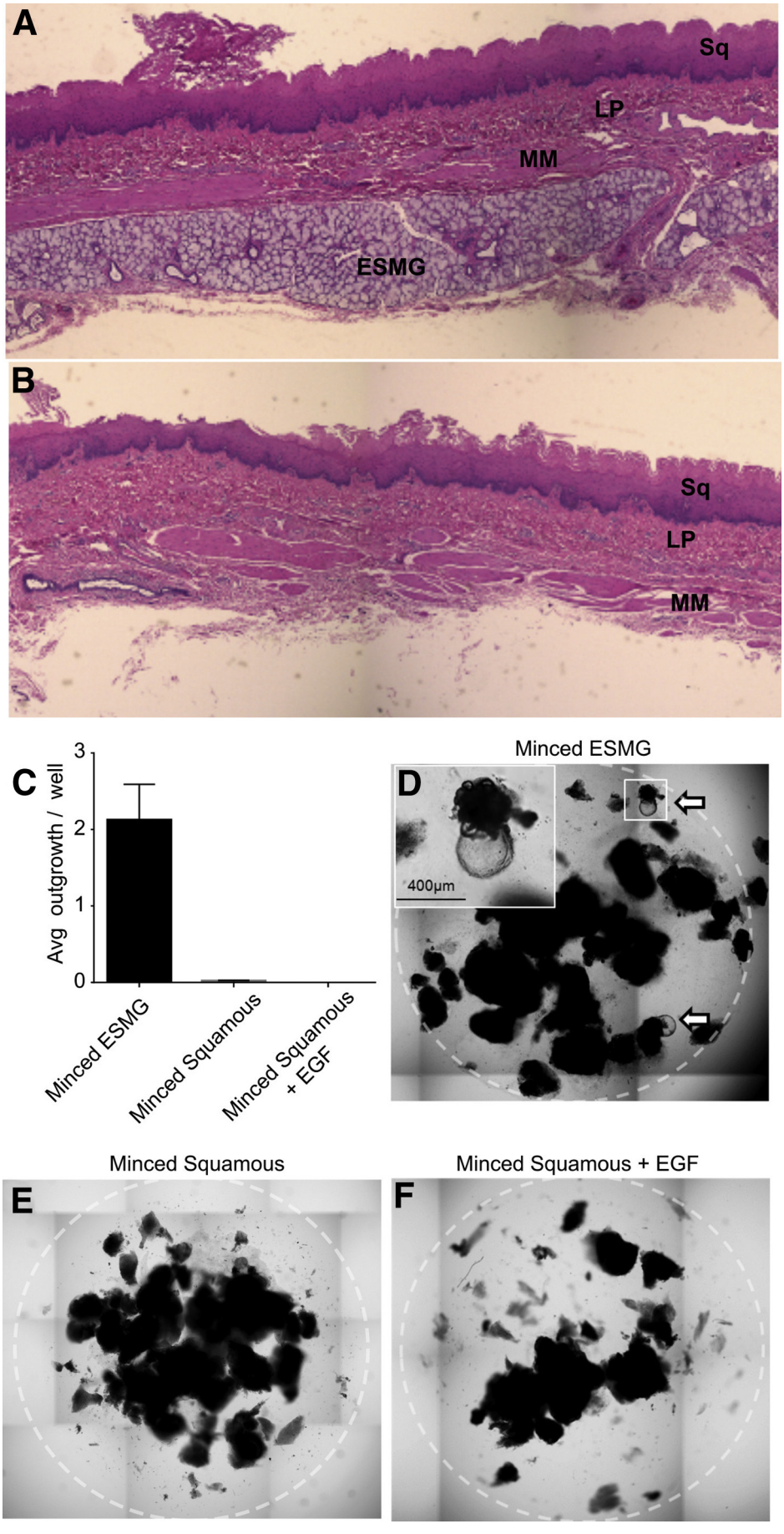

Figure 5. ESMG cells activate and proliferate in vitro after mincing. (*A*) ESMGs were present in the epithelial layer after it was peeled off the muscle layer. (*B*) ESMGs were dissected away from the muscularis mucosa, avoiding the squamous stem/progenitor cells and leaving the squamous layer intact. (*C*) Minced ESMGs formed an average of 2 outgrowths per well. (*D*) After 7 days, minced ESMGs produced new multicellular outgrowths as indicated with *arrows*. (*E*) In comparison and as a control, minced squamous epithelium did not produce outgrowths. (*F*) Addition of EGF to squamous culture conditions also did not produce outgrowths. Avg, average; LP, lamina propria; MM, muscularis mucosa; Sq, squamous.

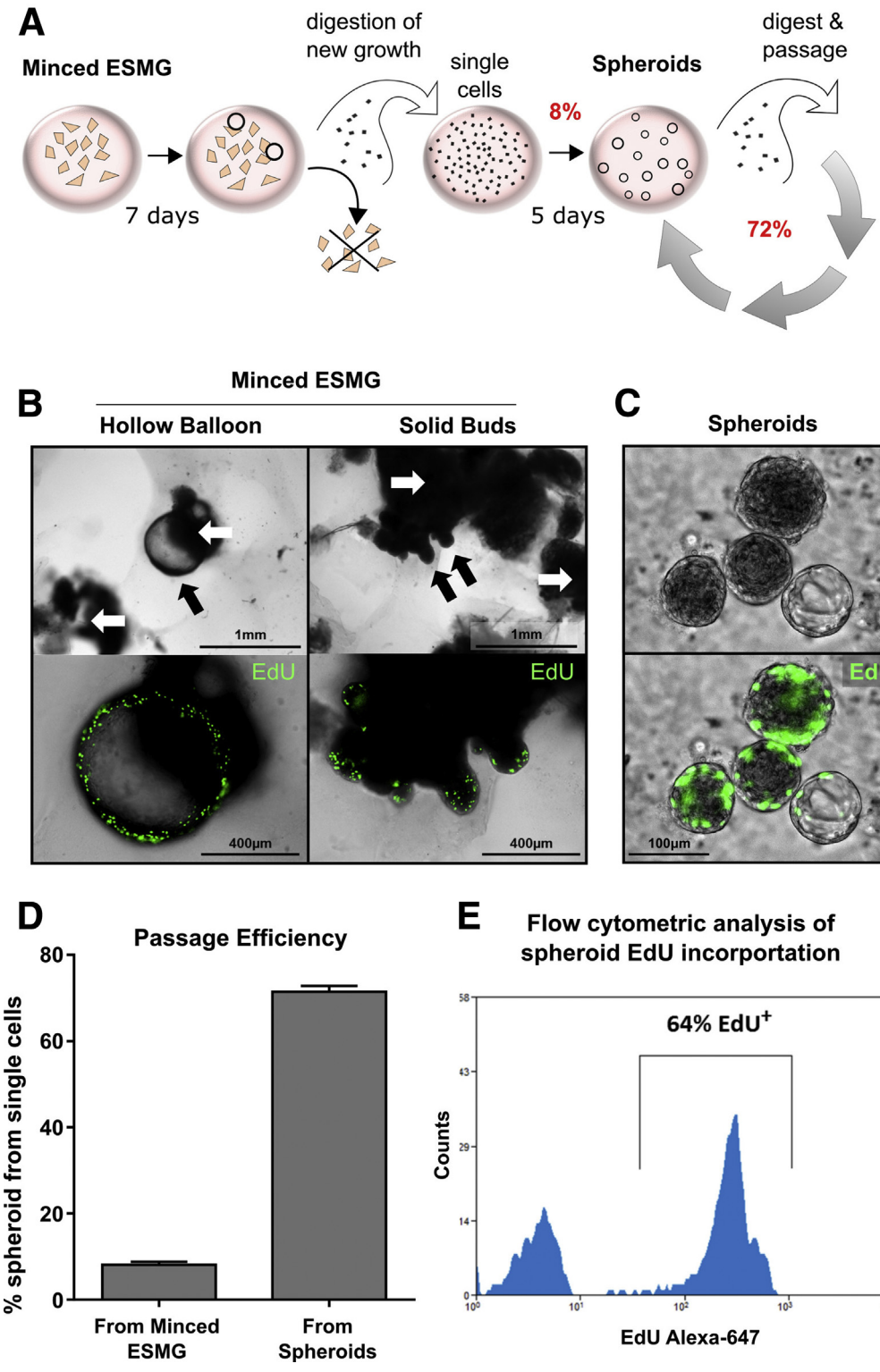

Figure 6. Digestion of minced ESMGs in culture yields proliferative spheroids. (*A*) After a gentle digestion, the single cells from the new growth were separated from their originating ESMG fragments and plated in growth factor–reduced Matrigel. These single cells formed multicellular spheroids that could be digested and passaged repeatedly. (*B*) Whole mount of minced outgrowths were both hollow and solid and both outgrowth types expressed EdU. *White arrows* indicate originating ESMG fragments and *black arrows* denote new outgrowths. (*C*) Digested outgrowths from minced ESMGs produced spheroids and examples of the spheroids are shown in whole mount with bright-field microscopy (*top*); the same spheroids are shown with fluorescence (*bottom*), where the spheroids showed extensive EdU positivity in green. (*D*) Cells (means ± SEM, 8% ± 0.6%) were passaged successfully from the minced ESMG-generated spheroids, and 72% ± 1% (means ± SEM) of cells subsequently passaged from spheroids reformed these multicellular units. (*E*) Edu-treated spheroids from 2 pigs were digested to single cells, pooled, and analyzed for EdU positivity by flow cytometry, 64% of the cells were EdU+.

literature (AGR2, MUC13, KRT18, MUC1, KRT8, and SOX9[32–34]) that were represented on the porcine microarray. We found increased expression of these BE markers in 3D culture of ESMG spheroids compared with squamous epithelium (Figure 8*C*), supporting the notion that cells within ESMGs have the potential to contribute to BE under certain conditions. We also compared expression of the BE markers between the ESMG spheroids and freshly dissected ESMGs. Interestingly, the same difference was not noted in expression of BE markers as was seen in

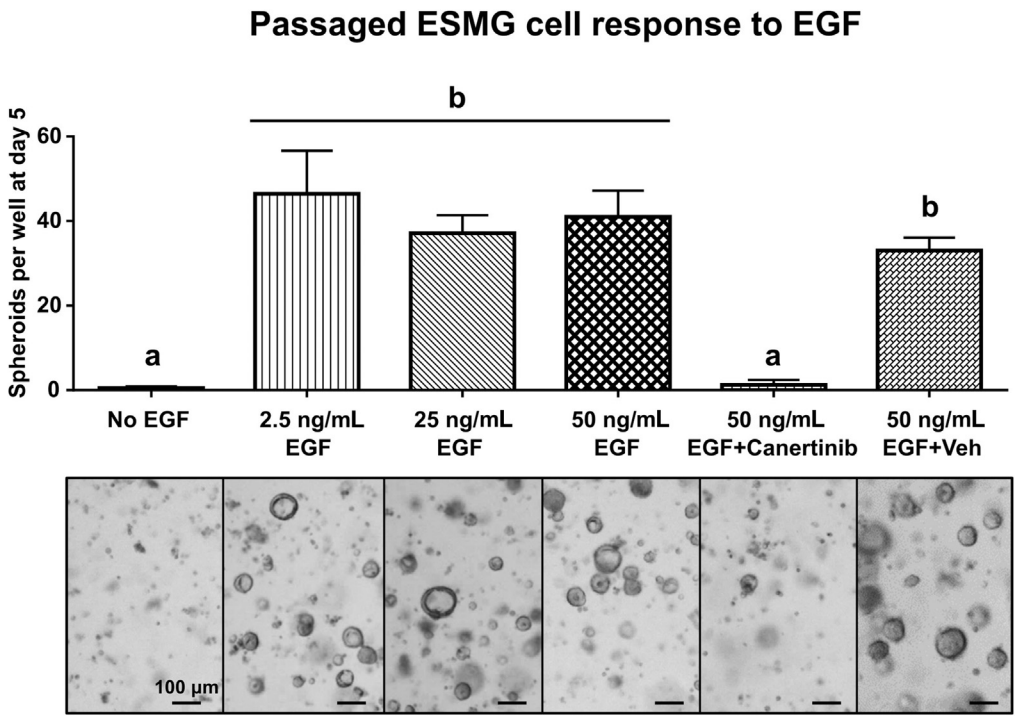

Figure 7. ESMG-derived spheroids are EGF-dependent. Spheroid formation from passaged cells was evaluated at day 5 after the following treatments: no EGF; 2.5 ng/mL recombinant EGF (rEGF); 25 ng/mL rEGF; 50 ng/mL rEGF; 50 ng/mL rEGF + canertinib (CI-1033), an irreversible pan-EGFR blocker; or 50 ng/mL rEGF with DMSO vehicle without the canertinib. The number of spheroids per well for the treatment groups was 0.5% ± 0.4%, 46% ± 10%, 37% ± 4%, 41% ± 6%, and 1.2% ± 1.2%, and 33% ± 3% for vehicle alone, means ± SEM respectively. Groups labeled under *a* are statistically significant from groups under *b* ($P < .05$; n = 3). Representative bright-field images are shown below the condition listed. Veh, vehicle without canertinib.

ESMG spheroids compared with squamous. MUC1 and MUC13 were increased in spheroids compared with fresh and uncultured ESMGs, but KRT8, KRT18, SOX9, and AGR2 were not significantly increased in spheroids vs ESMGs, whereas those BE markers all were increased in spheroids vs squamous tissue, highlighting similarly high expression of BE markers in both ESMGs and ESMG-derived spheroids.

Additional analysis of microarray data was performed to evaluate expression of known gastrointestinal stem cell markers in ESMG spheroids. Certain known stem cell markers such as LGR5, ASCL2, eR1, LRIG1, MSI1, and CDX1[35–37] were not represented on the porcine microarray. However, several other stem cell markers were present on the array and significantly enriched ($P < .05$) in ESMG spheroids when compared with squamous epithelium. For example, SOX9, a marker found in BE and in actively cycling intestinal stem cells as well as a reserve population was present in cultured ESMG spheroids with a 4.09-fold increase over squamous tissue.[38–40] OLFM4, another intestinal stem cell marker,[35,37,41] also was expressed in the ESMG spheroids with an 11.5-fold increase vs squamous tissue. Similarly, the gastric stem cell marker and chief cell marker MIST1 (official gene name BHLHA15)[42] was increased in ESMG spheroids vs squamous tissue with a fold change of 2.94. Other stem cell makers that we evaluated such as the esophageal and gastric marker SOX2, the gastric cancer stem cell markers CXCR4 and CD133,[36] the intestinal crypt marker and cell adhesion molecule CD166,[43] and BMI1, FKH6, or CDX2[44,45] were not increased in the ESMG spheroids compared with squamous tissue. None of the evaluated stem cell markers met significance when ESMG spheroids were compared with ESMGs. The complete list of differentially expressed genes for the ESMG spheroids vs squamous comparison and the ESMG spheroids vs freshly dissected ESMG comparison are provided in Supplementary Table 1.

Finally, lists of enriched genes (defined as at least 2-fold increased expression in ESMG spheroids with $P <$ .05) were created from the microarray comparisons of ESMG spheroids with squamous and ESMG spheroids with freshly dissected ESMGs. The ranked lists were subjected to PANTHER Classification for Pathway analysis. The results yielded 98 pathways of interest. The PANTHER rank of functionally classified pathways are shown in Table 2 and the entire PANTHER pathway list is provided in Supplementary Table 2. Of particular note is the fact that hedgehog signaling, EGF receptor signaling, and transforming growth factor-β signaling ranked within the top 5 of both lists (from ESMG spheroids to squamous as well as ESMG spheroids to freshly dissected ESMGs). Notch, Wnt signaling, and fibroblast growth factor signaling were enriched in both lists, but with markedly lower ranks.

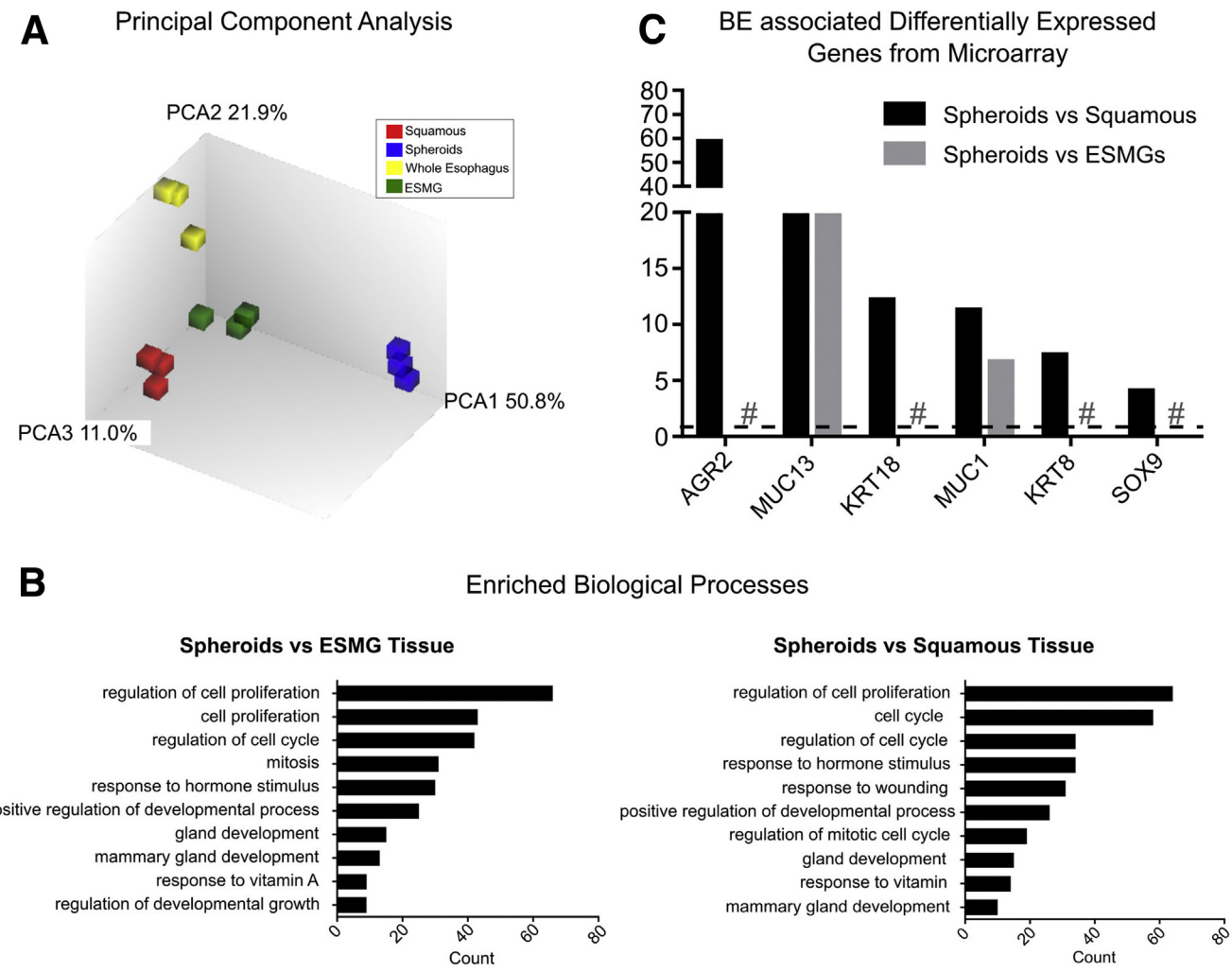

Figure 8. ESMG-derived spheroids show a unique transcriptomic signature and increased expression of BE-associated genes by microarray. (*A*) Principal component analysis (PCA) plot of microarray data comparing squamous epithelium, ESMGs, spheroids generated from ESMGs in 3D culture, and whole uninjured porcine esophagus show distinct clusters for each group. Importantly, the activated ESMG spheroids in culture assume a unique profile distinct from ESMGs of origin. (*B*) Biologic processes gene ontology analysis using the Database for Annotation showed that cultured spheroids compared with squamous epithelium and cultured spheroids in culture compared with freshly dissected ESMGs showed increased cell proliferation, cell-cycle markers, hormone responses, and gland development. The ESMGs in culture compared with squamous also showed responses to wound healing, reflecting their activated state in culture. (*C*) Established BE markers represented on the porcine microarray were assessed in spheroids in 3D culture compared with squamous epithelium and showed increased expression of several known BE markers including AGR2, MUC13, KRT18, MUC1, KRT8, and SOX9. Only MUC13 and MUC1 were increased in ESMG spheroid culture compared with dissected ESMGs. *Hash marks* show where there was no significant difference in expression between ESMG spheroid culture and freshly dissected ESMGs.

Two Phenotypes of Spheroids Arise From ESMGs

In each ESMG preparation, once the spheroids formed, we observed a mix of 2 spheroid phenotypes (Figure 9*A* and *B*). One phenotype was solid in appearance, resembling squamous epithelium, whereas the other was hollow with the cells assuming a cuboidal ductal appearance. Whole-mount staining then was used to immunolabel spheroids for CK7 and P63, markers of ductal cells and BE (CK7) and squamous cells (P63). This labeling showed different patterns of staining for the 2 types of spheroids (Figure 9*C* and *D*). The solid spheroids were P63+, similar to the basal layer of normal squamous epithelium, whereas the hollow spheroids expressed CK7, which is found in ESMG ducts and in BE but not in normal squamous epithelium.

Although some experimental variation exists in the proportion of solid/squamous and hollow/ductal spheroids, both phenotypes were consistently present after the first passage and after subsequent passages. At 7 days after passaging, the spheroids (ie, the mixture of both phenotypes) were digested to single cells, fixed, and labeled with CK7 and P63. When labeled cells from this cell suspension were viewed under a fluorescent microscope, it was visually evident that CK7 and P63 antibodies were mutually

Table 2. PANTHER Pathway Rank

Rank	Pathway name
Selected examples: spheroids vs squamous	
1	Corticotropin-releasing factor–receptor signaling pathway
2	Hedgehog signaling pathway
3	Androgen/estrogen/progesterone biosynthesis
4	EGF-receptor signaling pathway
5	TGF-β signaling pathway
15	JAK/STAT signaling pathway
26	Insulin/IGF pathway MAP kinase kinase/MAP kinase cascade
38	Notch signaling pathway
53	Ras pathway
61	Wnt signaling pathway
66	FGF signaling pathway
77	p53 pathway
90	PI3 kinase pathway
Selected examples: spheroids vs ESMGs	
1	Corticotropin-releasing factor–receptor signaling pathway
2	Hedgehog signaling pathway
3	Androgen/estrogen/progesterone biosynthesis
4	EGF-receptor signaling pathway
5	TGF-β signaling pathway
14	JAK/STAT signaling pathway
23	Insulin/IGF pathway MAP kinase kinase/MAP kinase cascade
34	Notch signaling pathway
47	Ras pathway
55	Wnt signaling pathway
61	FGF signaling pathway
72	p53 pathway
84	PI3 kinase pathway

FGF, fibroblast growth factor; IGF, insulin-like growth factor; JAK/STAT, Janus kinase/signal transducers and activators of transcription; MAP, mitogen-activated protein; PI3, phosphatidylinositol 3; TGF, transforming growth factor.

exclusive (Figure 9*E*). Flow cytometry confirmed that CK7 and P63 identify largely distinct populations of cells. Although we expect the proportion of CK7 and P63 cells to vary based on the ratio of phenotypes, overall flow cytometry results indicated that approximately 90% of cells express either CK7 or P63 (Figure 9*F*).

Discussion

Although previous histologic studies have associated ESMGs and ducts with outgrowths of both squamous epithelium and BE, functional studies to determine the cellular and molecular mechanisms that link ESMGs and epithelial repair have been lacking. In addition, the potential for proliferative response of ESMGs to epithelial injury represents an important finding. A major reason why such studies have not been performed is the absence of ESMGs in popular animal models (eg, mice) most commonly used for research. Although a porcine in vivo model is relevant, in vivo studies with pigs are quite expensive and can be performed only at institutions with large animal facilities. Development of a new in vitro culture model using primary porcine tissue therefore seemed imperative. In this alternative approach, our cell culture model of ESMGs provides a novel way to expand our understanding of esophageal repair. We have developed this 3D porcine culture model of ESMGs in an effort to explore the proliferative capacity and phenotypic potential of the gland's resident cells.

To develop this model, we first compared histology of pig and human esophagus and determined that ESMGs in porcine and human esophagus are of similar size and composition. Expression of the ductal/BE marker CK7 and the basal squamous marker P63 were also similar between pig and human esophagus in vivo. These markers then were used for the phenotypic evaluation of the cell culture model.

As an initial step in establishing the ESMG model, the proliferative capacity of these glands was evaluated. Previous human studies have shown a proliferative compartment in the basal layer of the squamous epithelium with turnover approximately every 11 days.[15] Those human studies were performed by administering bromodeoxyuridine or iododeoxyuridine to patients before esophagectomy.[2,15] In comparison with the squamous epithelium, ESMGs were not proliferative at baseline, with no thymidine analog uptake noted in the human ESMGs in the uninjured state.[2] Our PCNA staining (Figure 2) confirmed minimal proliferation in control ESMGs. In contrast, we observed extensive proliferation in ESMGs with acinar ductal metaplasia. After administering EdU to a healthy pig, we found a similar pattern in the porcine esophagus with very scant uptake of EdU in the ESMGs. However, after esophageal injury, porcine ESMGs with a ductal phenotype showed a significant increase in EdU labeling. The ductal phenotype within ESMGs after injury was similar to what we previously reported in human ESMGs after esophageal injury.[11] Specifically, in our human studies, acinar ductal metaplasia in ESMGs was most intense in areas directly under areas of epithelial ulceration in human beings.[11] The finding of ESMG activation in association with injury provide a logical framework for the ESMG culture experiments presented here.

Although dissecting ESMGs, mincing them, and placing them in Matrigel is different from what occurs during in vivo epithelial injury, both conditions induce proliferation. In culture, balloon-like outgrowths emerged from minced ESMGs and as we passaged these outgrowths, spheroids formed with high efficiency. The evoked proliferative response of ESMG-derived cells in vitro was documented by active incorporation of EdU into growing spheroids. This points to the possibility that ESMGs may represent a protected source of progenitor cells that specifically respond to significant esophageal injury.

In contrast to previous reports of esophageal culture, the initial outgrowths from minced ESMGs in Matrigel did not require exogenous growth factors, likely owing to intrinsic production of EGF and possibly other factors produced by

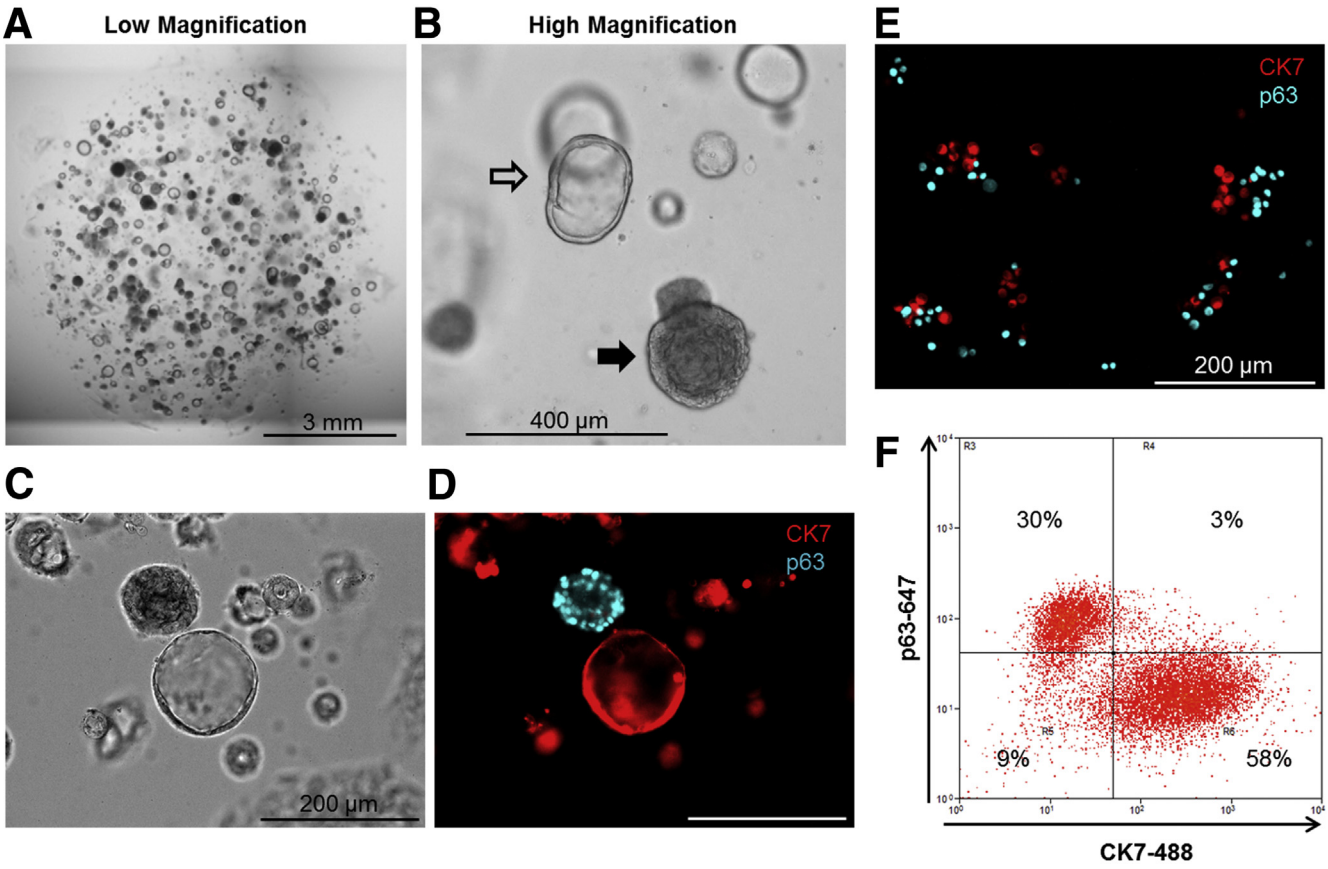

Figure 9. Spheroids generated from ESMGs develop 2 distinct phenotypes. (*A*) With a 4× objective, a mix of the 2 spheroid phenotypes can be observed. (*B*) A higher-power bright-field image of a ductal (*hollow arrow*) and a squamous (*solid arrow*) phenotype are shown. (*C* and *D*) One spheroid phenotype (ductal) is characterized by the CK7 marker found in ESMGs and ducts as well as in Barrett's esophagus (BE) and the other spheroid phenotype is characterized by P63, a known squamous marker that is lost in BE. (*E*) Single cells isolated from spheroids fixed and labeled with antibodies against CK7 (red) and P63 (blue) viewed under a wide-field fluorescent microscope. (*F*) Cells from the same preparation shown in panel *E* evaluated by flow cytometry and represented on a bivariate histogram.

the ESMGs themselves. After passage of cells from new growth and removal of their originating fragments, ESMG cultures became EGF-dependent, but required relatively minimal media compared with culture of intestinal epithelium or superficial esophageal epithelium.[46,47] Prior in vivo studies of human esophagus have shown that EGF is critical for the integrity of the esophageal epithelium, and basal levels of EGF secretion from ESMGs yield luminal concentrations in the range of 2 ng/mL.[30] EGF also is stable even in an acidic environment, supporting its role in esophageal repair after acid-induced injury.[30] In our dose-titration experiments (Figure 7), ESMG cultures respond equally to 2.5 ng/mL EGF (approximating physiologic levels) and 50 ng/mL EGF, which we adapted from the widely used intestinal epithelial cell culture conditions developed by Sato and Clevers.[31] This consistent and robust response to low EGF concentrations in culture suggests the cells are exquisitely sensitive to this growth factor.

In human beings, ESMGs have been described in continuity with both types of adult esophageal epithelium: squamous and BE epithelium.[7,8] In the current work, when grown in culture, cells derived from ESMGs produced 2 distinct and separate phenotypes: a hollow ductal spheroid that, similar to BE, is CK7+, and a solid squamous spheroid that, similar to squamous epithelium, is P63+. The observation of dual phenotypes is distinct from prior esophageal culture models.[46,47] Spheroids from esophageal squamous epithelium were solid in appearance and P63+, similar to the solid P63+ spheroids in our ESMG cultures.[46] In contrast, BE cultures formed cystic structures with a hollow appearance,[47] similar to the hollow ductal spheroids derived from our ESMG cultures. Interestingly, a report of a multipotent luminal progenitor yielding very similar dual hollow and solid organoid phenotypes has been described in human prostate gland cultures.[48] Similar to ESMG-derived spheroids, EGF also was found to be essential for prostate gland organoid culture.[48]

Central to furthering our knowledge of the development of BE and esophageal carcinogenesis is the question of potential sources of esophageal stem cells. Currently, it is known that basal cells within the squamous epithelium serve as a source of progenitor cells to replenish the squamous esophagus.[49–51] In the setting of localized injury, basal cells within the squamous epithelium respond, and

homeostasis quickly returns to the esophagus.[51] It is worth noting that in our model, minced squamous epithelium with adherent lamina propria did not grow in minimal media conditions, suggesting a self-sufficiency inherent to the glands. In addition, this lack of growth from squamous epithelium makes it very unlikely that the squamous phenotype we observed from ESMGs was a result of squamous contamination. Our data suggest that ESMGs may contain a population of stem cells that are typically quiescent, or slowly cycling, but capable of rapid proliferation after significant injury, a concept supported in the stem cell literature.[39,51] In our gene expression analysis, although certain stem cell markers from the stomach and intestine were present in ESMG spheroids compared with squamous, including SOX9, OLFM4, and MIST1, other stem cell markers were not highly expressed. This could be in part because the ESMG spheroids are already highly proliferative in marked contrast to ESMGs in uninjured esophagus. A population of cells in ESMGs with plasticity and proliferative potential might be needed in the setting of major esophageal injury where large areas of esophageal epithelium are lost, such as in severe erosive esophagitis or after ablative therapy for BE.

The microarray analysis results also support that ESMG spheroids express BE markers when compared with squamous tissue. The fact that ESMGs in culture and fresh ESMGs do not differ in the expression of several important BE markers such as AGR2, KRT18, KRT8, and SOX9 supports the common expression of BE markers in ESMGs rather than squamous epithelium.

Studies of clonality have suggested that ESMG ducts may produce both squamous epithelium and BE.[9] Specifically, normal squamous islands within a field of mutation-carrying BE shared clonality with wild-type ESMG gland ducts. In addition, a single point mutation in the ESMG duct also was present in adjacent BE, strongly pointing to a common clonal origin.[9] Although esophageal biopsy specimens only survive in culture for 48 hours, columnar epithelium appeared to emerge from ESMGs.[10] Given the clonal and culture data from human esophagus, it is thus particularly interesting that ESMGs in culture produced 2 phenotypes of spheroids similar to both previously cultured BE and squamous epithelium, supporting the notion that ESMGs could contribute to both normal esophageal repair of squamous epithelium or repopulation of an injured esophagus with a columnar BE phenotype. This type of abnormal repair was described in human beings by Adler[52] in 1963, in which, after repeated bouts of esophageal injury and repair, squamous esophagus was replaced by simple columnar epithelium. Similar to human beings and pigs, the canine esophagus contains ESMGs. When a ring of squamous epithelium was removed from the distal esophagus in dogs, columnar epithelium filled the defect.[53] This columnar epithelium was noted to occur directly above ESMGs and in direct continuity with the cuboidal epithelium of a duct leading from an ESMG.[53]

Although we have learned that ESMGs harbor a proliferative potential, it remains unknown what specific populations of cells in ESMGs possess this ability to proliferate in response to injury. The conceptual framework of cellular plasticity and reserve stem cells emerging in the setting of injury relates to our observation of acinar ductal metaplasia in human ESMGs.[11] Our results indicate the possibility that ESMGs could serve as a source of cells for repair, and the literature suggests several possibilities for where the cells with proliferative potential reside. Although not the focus of our current study, P63+ cells adjacent to the ducts and circumscribing the acini could be studied as a source of proliferative cells.[17] In the pseudostratified epithelium of the prostate ducts, P63+ basal cells within the glands have shown the ability to generate a complete prostate gland in vitro.[48] In an in vivo lineage tracing study in prostate, a rare P63+ basal cell population in mice has been shown to be bi-potential, giving rise to both basal and luminal cells.[54] Additional research is needed to isolate and characterize analogous subpopulations from ESMGs including the acinar cells, peri-acinar myofibroblasts, and the ductal epithelium.

Pathway analysis based on gene expression data from ESMG spheroids compared with squamous tissue or ESMGs yielded similar results with several expected pathways such as EGF-receptor signaling, as we found in our EGF-dependent cultures. Hedgehog signaling was shown as an important pathway, and although hedgehog signaling is not present in adult squamous tissue, it has been associated with the development of BE.[55] Further investigation is needed into signaling pathways that are active after esophageal injury and associated with ESMG proliferation.

It remains unclear if the hollow/ductal and solid/squamous phenotypes of spheroids from ESMGs are committed or plastic, and future research will address this important question. Our group is actively developing methods to separate and characterize the 2 phenotypes of spheroids from the ESMG cultures. This will allow us to assess the plasticity as well as the gene expression profiles of each phenotype. In addition, the clinical exposures associated with esophageal acinar ductal metaplasia in ESMGs remain unknown. This 3D cell culture model will allow us to study the effects of these exposures in a prospective manner not feasible in human beings or large animals. We expect this model may yield insights into the mechanisms that drive the development of acinar ductal metaplasia in the esophagus, an important line of research given the association of esophageal acinar ductal metaplasia with BE and EAC.

References

1. Shi L, Der R, Ma Y, Peters J, Demeester T, Chandrasoma P. Gland ducts and multilayered epithelium in mucosal biopsies from gastroesophageal-junction region are useful in characterizing esophageal location. Dis Esophagus 2005;18:87–92.
2. van Nieuwenhove Y, Destordeur H, Willems G. Spatial distribution and cell kinetics of the glands in the human esophageal mucosa. Eur J Morphol 2001;39:163–168.
3. Mills JC, Sansom OJ. Reserve stem cells: differentiated cells reprogram to fuel repair, metaplasia, and neoplasia in the adult gastrointestinal tract. Sci Signal 2015;8:re8.

4. McDonald SAC, Graham TA, Lavery DL, Wright NA, Jansen M. The Barrett's gland in phenotype space. Cell Mol Gastroenterol Hepatol 2015;1:41–54.
5. Howlader N, Noone AM, Krapcho M, Garshell J, Neymann N, Altekruse SF, Kosary CL, Yu M, Ruhl J, Tatalovich Z, Mariotto A, Lewis DR, Chen HS, Feuer EJ, Cronin KA, eds. SEER cancer statistics review, 1975-2011 Bethesda, MD: National Cancer Institute; 2014 based on November 2013 SEER data submission, posted to the SEER web site, April 4. Available from: http://seer.cancer.gov/csr/1975_2011. Accessed October 17, 2014.
6. Pohl H, Welch HG. The role of overdiagnosis and reclassification in the marked increase of esophageal adenocarcinoma incidence. J Natl Cancer Inst 2005; 97:142–146.
7. Coad RA, Woodman AC, Warner PJ, Barr H, Wright NA, Shepherd NA. On the histogenesis of Barrett's oesophagus and its associated squamous islands: a three-dimensional study of their morphological relationship with native oesophageal gland ducts. J Pathol 2005; 206:388–394.
8. Lorinc E, Oberg S. Submucosal glands in the columnar-lined oesophagus: evidence of an association with metaplasia and neosquamous epithelium. Histopathology 2012;61:53–58.
9. Leedham SJ, Preston SL, McDonald SA, Elia G, Bhandari P, Poller D, Harrison R, Novelli MR, Jankowski JA, Wright NA. Individual crypt genetic heterogeneity and the origin of metaplastic glandular epithelium in human Barrett's oesophagus. Gut 2008; 57:1041–1048.
10. Chang CL, Lao-Sirieix P, Save V, De La Cueva Mendez G, Laskey R, Fitzgerald RC. Retinoic acid-induced glandular differentiation of the oesophagus. Gut 2007;56:906–917.
11. Garman KS, Kruger L, Thomas S, Swiderska-Syn M, Moser BK, Diehl AM, McCall SJ. Ductal metaplasia in oesophageal submucosal glands is associated with inflammation and oesophageal adenocarcinoma. Histopathology 2015;67:771–782.
12. Strobel O, Rosow DE, Rakhlin EY, Lauwers GY, Trainor AG, Alsina J, Fernandez-Del Castillo C, Warshaw AL, Thayer SP. Pancreatic duct glands are distinct ductal compartments that react to chronic injury and mediate Shh-induced metaplasia. Gastroenterology 2010;138:1166–1177.
13. Shi G, DiRenzo D, Qu C, Barney D, Miley D, Konieczny SF. Maintenance of acinar cell organization is critical to preventing Kras-induced acinar-ductal metaplasia. Oncogene 2013;32:1950–1958.
14. Garman KS, Orlando RC, Chen X. Review: experimental models for Barrett's esophagus and esophageal adenocarcinoma. Am J Physiol Gastrointest Liver Physiol 2012; 302:G1231–G1243.
15. Pan Q, Nicholson AM, Barr H, Harrison LA, Wilson GD, Burkert J, Jeffery R, Alison MR, Looijenga L, Lin WR, McDonald SA, Wright NA, Harrison R, Peppelenbosch MP, Jankowski JA. Identification of lineage-uncommitted, long-lived, label-retaining cells in healthy human esophagus and stomach, and in metaplastic esophagus. Gastroenterology 2013;144:761–770.
16. Geddert H, Kiel S, Heep HJ, Gabbert HE, Sarbia M. The role of p63 and deltaNp63 (p40) protein expression and gene amplification in esophageal carcinogenesis. Hum Pathol 2003;34:850–856.
17. Glickman JN, Yang A, Shahsafaei A, McKeon F, Odze RD. Expression of p53-related protein p63 in the gastrointestinal tract and in esophageal metaplastic and neoplastic disorders. Hum Pathol 2001; 32:1157–1165.
18. Daniely Y, Liao G, Dixon D, Linnoila RI, Lori A, Randell SH, Oren M, Jetten AM. Critical role of p63 in the development of a normal esophageal and tracheobronchial epithelium. Am J Physiol Cell Physiol 2004; 287:C171–C181.
19. Kruger L, Gonzalez LM, von Furstenberg RJ, Henning SJ, Blikslager A, Garman KS. Ductular and proliferative response of esophageal submucosal glands in a porcine model of esophageal injury and repair. Gastroenterology 2016;150:S679–S680.
20. Kruger L, Gonzalez LM, Pridgen TA, McCall SJ, von Furstenberg R, Harnden I, Carnighan GE, Cox AM, Blikslager AT, Garman KS. Ductular and proliferative response of esophageal submucosal glands in a porcine model of esophageal injury and repair. Am J Physiol Gastrointest Liver Physiol 2017, Epub ahead of print.
21. Reznikov EA, Comstock SS, Yi C, Contractor N, Donovan SM. Dietary bovine lactoferrin increases intestinal cell proliferation in neonatal piglets. J Nutr 2014; 144:1401–1408.
22. Sarosiek J, Feng T, McCallum RW. The interrelationship between salivary epidermal growth factor and the functional integrity of the esophageal mucosal barrier in the rat. Am J Med Sci 1991;302:359–363.
23. Wang L, Brugge JS, Janes KA. Intersection of FOXO- and RUNX1-mediated gene expression programs in single breast epithelial cells during morphogenesis and tumor progression. Proc Natl Acad Sci 2011; 108:E803–E812.
24. Mi H, Dong Q, Muruganujan A, Gaudet P, Lewis S, Thomas PD. PANTHER version 7: improved phylogenetic trees, orthologs and collaboration with the Gene Ontology Consortium. Nucleic Acids Res 2010; 38:D204–D210.
25. Thomas PD, Campbell MJ, Kejariwal A, Mi H, Karlak B, Daverman R, Diemer K, Muruganujan A, Narechania A. PANTHER: a library of protein families and subfamilies indexed by function. Genome Res 2003;13:2129–2141.
26. Glickman JN, Ormsby AH, Gramlich TL, Goldblum JR, Odze RD. Interinstitutional variability and effect of tissue fixative on the interpretation of a Barrett cytokeratin 7/20 immunoreactivity pattern in Barrett esophagus. Hum Pathol 2005;36:58–65.
27. Abdulnour-Nakhoul S, Nakhoul NL, Wheeler SA, Haque S, Wang P, Brown K, Orlando G, Orlando RC. Characterization of esophageal submucosal glands in pig tissue and cultures. Dig Dis Sci 2007;52:3054–3065.

28. Glickman JN, Chen YY, Wang HH, Antonioli DA, Odze RD. Phenotypic characteristics of a distinctive multilayered epithelium suggests that it is a precursor in the development of Barrett's esophagus. Am J Surg Pathol 2001;25:569–578.
29. Sato T, Vries RG, Snippert HJ, van de Wetering M, Barker N, Stange DE, van Es JH, Abo A, Kujala P, Peters PJ, Clevers H. Single Lgr5 stem cells build crypt-villus structures in vitro without a mesenchymal niche. Nature 2009;459:262–265.
30. Sarosiek J, Hetzel DP, Yu Z, Piascik R, Li L, Rourk RM, McCallum RW. Evidence on secretion of epidermal growth factor by the esophageal mucosa in humans. Am J Gastroenterol 1993;88:1081–1087.
31. Sato T, Clevers H. Primary mouse small intestinal epithelial cell cultures. Methods Mol Biol 2013; 945:319–328.
32. Stairs DB, Nakagawa H, Klein-Szanto A, Mitchell SD, Silberg DG, Tobias JW, Lynch JP, Rustgi AK. Cdx1 and c-Myc foster the initiation of transdifferentiation of the normal esophageal squamous epithelium toward Barrett's esophagus. PLoS One 2008;3:e3534.
33. Pohler E, Craig AL, Cotton J, Lawrie L, Dillon JF, Ross P, Kernohan N, Hupp TR. The Barrett's antigen anterior gradient-2 silences the p53 transcriptional response to DNA damage. Mol Cell Proteomics 2004; 3:534–547.
34. Nakagawa H, Whelan K, Lynch JP. Mechanisms of Barrett's oesophagus: intestinal differentiation, stem cells, and tissue models. Best Pract Res Clin Gastroenterol 2015;29:3–16.
35. Barker N, van Es JH, Kuipers J, Kujala P, van den Born M, Cozijnsen M, Haegebarth A, Korving J, Begthel H, Peters PJ, Clevers H. Identification of stem cells in small intestine and colon by marker gene Lgr5. Nature 2007;449:1003–1007.
36. Demitrack ES, Samuelson LC. Notch as a driver of gastric epithelial cell proliferation. Cell Mol Gastroenterol Hepatol 2017;3:323–330.
37. van der Flier LG, van Gijn ME, Hatzis P, Kujala P, Haegebarth A, Stange DE, Begthel H, van den Born M, Guryev V, Oving I, van Es JH, Barker N, Peters PJ, van de Wetering M, Clevers H. Transcription factor achaete scute-like 2 controls intestinal stem cell fate. Cell 2009; 136:903–912.
38. Clemons NJ, Wang DH, Croagh D, Tikoo A, Fennell CM, Murone C, Scott AM, Watkins DN, Phillips WA. Sox9 drives columnar differentiation of esophageal squamous epithelium: a possible role in the pathogenesis of Barrett's esophagus. Am J Physiol Gastrointest Liver Physiol 2012;303:G1335–G1346.
39. Henning SJ, von Furstenberg RJ. GI stem cells - new insights into roles in physiology and pathophysiology. J Physiol 2016;594:4769–4779.
40. Roche KC, Gracz AD, Liu XF, Newton V, Akiyama H, Magness ST. SOX9 maintains reserve stem cells and preserves radioresistance in mouse small intestine. Gastroenterology 2015;149:1553–1563 e10.
41. VanDussen KL, Carulli AJ, Keeley TM, Patel SR, Puthoff BJ, Magness ST, Tran IT, Maillard I, Siebel C, Kolterud A, Grosse AS, Gumucio DL, Ernst SA, Tsai YH, Dempsey PJ, Samuelson LC. Notch signaling modulates proliferation and differentiation of intestinal crypt base columnar stem cells. Development 2012;139: 488–497.
42. Hayakawa Y, Fox JG, Wang TC. The origins of gastric cancer from gastric stem cells: lessons from mouse models. Cell Mol Gastroenterol Hepatol 2017;3: 331–338.
43. Smith NR, Davies PS, Levin TG, Gallagher AC, Keene DR, Sengupta SK, Wieghard N. El Rassi E, Wong MH. Cell adhesion molecule CD166/ALCAM functions within the crypt to orchestrate murine intestinal stem cell homeostasis. Cell Mol Gastroenterol Hepatol 2017; 3:389–409.
44. Reinisch C, Kandutsch S, Uthman A, Pammer J. BMI-1: a protein expressed in stem cells, specialized cells and tumors of the gastrointestinal tract. Histol Histopathol 2006;21:1143–1149.
45. Yen TH, Wright NA. The gastrointestinal tract stem cell niche. Stem Cell Rev 2006;2:203–212.
46. Jeong Y, Rhee H, Martin S, Klass D, Lin Y, Nguyen LX, Feng W, Diehn M. Identification and genetic manipulation of human and mouse oesophageal stem cells. Gut 2016; 65:1077–1086.
47. Sato T, Stange DE, Ferrante M, Vries RG, Van Es JH, Van den Brink S, Van Houdt WJ, Pronk A, Van Gorp J, Siersema PD, Clevers H. Long-term expansion of epithelial organoids from human colon, adenoma, adenocarcinoma, and Barrett's epithelium. Gastroenterology 2011;141:1762–1772.
48. Karthaus WR, Iaquinta PJ, Drost J, Gracanin A, van Boxtel R, Wongvipat J, Dowling CM, Gao D, Begthel H, Sachs N, Vries RG, Cuppen E, Chen Y, Sawyers CL, Clevers HC. Identification of multipotent luminal progenitor cells in human prostate organoid cultures. Cell 2014;159:163–175.
49. Seery JP, Watt FM. Asymmetric stem-cell divisions define the architecture of human oesophageal epithelium. Curr Biol 2000;10:1447–1450.
50. Kalabis J, Oyama K, Okawa T, Nakagawa H, Michaylira CZ, Stairs DB, Figueiredo JL, Mahmood U, Diehl JA, Herlyn M, Rustgi AK. A subpopulation of mouse esophageal basal cells has properties of stem cells with the capacity for self-renewal and lineage specification. J Clin Invest 2008;118:3860–3869.
51. Doupe DP, Alcolea MP, Roshan A, Zhang G, Klein AM, Simons BD, Jones PH. A single progenitor population switches behavior to maintain and repair esophageal epithelium. Science 2012;337:1091–1093.
52. Adler RH. The lower esophagus lined by columnar epithelium. Its association with hiatal hernia, ulcer, stricture, and tumor. J Thorac Cardiovasc Surg 1963; 45:13–34.
53. Gillen P, Keeling P, Byrne PJ, West AB, Hennessy TP. Experimental columnar metaplasia in the canine oesophagus. Br J Surg 1988;75:113–115.
54. Wang ZA, Mitrofanova A, Bergren SK, Abate-Shen C, Cardiff RD, Califano A, Shen MM. Lineage analysis of basal epithelial cells reveals their unexpected plasticity

and supports a cell-of-origin model for prostate cancer heterogeneity. Nat Cell Biol 2013;15:274–283.

55. Wang DH, Clemons NJ, Miyashita T, Dupuy AJ, Zhang W, Szczepny A, Corcoran-Schwartz IM, Wilburn DL, Montgomery EA, Wang JS, Jenkins NA, Copeland NA, Harmon JW, Phillips WA, Watkins DN. Aberrant epithelial-mesenchymal Hedgehog signaling characterizes Barrett's metaplasia. Gastroenterology 2010;138:1810–1822.

Received March 16, 2017. Accepted July 13, 2017.

Correspondence
Address correspondence to: Katherine S. Garman, MD, Division of Gastroenterology, Department of Medicine, Duke University Medical Center, Box 3913, Durham, North Carolina 27710. e-mail: katherine.garman@duke.edu; fax: (919) 684-4983.

Acknowledgments
The authors would like to thank City Packing, in particular Thomas McGarity and Jamie Corbett, for their generous contributions of porcine esophagus; Thomas C. Becker, PhD, for edits; Solange Abdoulnour-Najhoul, PhD for guidance localizing and visualizing porcine ESMGs in dissection; and Xiaoxin L. Chen, MD, PhD, and Roy G. Orlando, MD, for thoughtful discussion and intellectual contributions. In addition, the authors acknowledge and thank the Biospecimen Repository and Processing Core, a shared resource of the Duke University School of Medicine and Duke Cancer Institute, for providing access to the human biospecimens used under Institutional Review Board oversight in this work.

Author contributions
Richard J. von Furstenberg was responsible for the experimental design, data acquisition, and analysis including statistical analysis, and drafting the manuscript; Joy Li and Cristina Stolarchuk were responsible for data acquisition, analysis, and interpretation; Rachel Feder was responsible for data analysis and interpretation; Alexa Campbell was responsible for data acquisition, analysis, and interpretation; Leandi Kruger was responsible for porcine in vivo experiments and data acquisition including immunohistochemistry; Liara M. Gonzalez was responsible for the experimental design, porcine in vivo experiments, and technical and material support; Anthony T. Blikslager was responsible for the experimental design, porcine in vivo experiments, funding, and material support; Diana M. Cardona and Shannon J. McCall were responsible for histologic analysis and interpretation; Susan J. Henning was responsible for the experimental design, data interpretation, and critical manuscript edits; and Katherine S. Garman was responsible for the study concept, funding, experimental design and analysis, drafting of the manuscript, and study supervision.

Conflicts of interest
The authors disclose no conflicts.

Funding
Supported by National Institutes of Health grants K08-DK098528 (K.S.G.) and P30-DK034987 (K.S.G. and A.T.B.), for the Center for Gastrointestinal Biology and Disease via the Large Animal Models Core at North Carolina State University (Large Animal Models Core to A.T.B. and L.M.G.). The Biospecimen Repository and Processing Core receives support from the P30 Cancer Center support grant (P30 CA014236).